Perspective: Ga$_2$O$_3$ for ultra-high power rectifiers and MOSFETS (F)

(ID) **S. J. Pearton**, (ID) **Fan Ren, Marko Tadjer, et al.**

COLLECTIONS

(F)   This paper was selected as Featured

View Online   Export Citation   CrossMark

ARTICLES YOU MAY BE INTERESTED IN

Demonstration of β–(Al$_x$Ga$_{1-x}$)$_2$O$_3$/Ga$_2$O$_3$ double heterostructure field effect transistors
Applied Physics Letters **112**, 233503 (2018); https://doi.org/10.1063/1.5037095

Halide vapor phase epitaxial growth of β-Ga$_2$O$_3$ and α-Ga$_2$O$_3$ films
APL Materials **7**, 022504 (2019); https://doi.org/10.1063/1.5055680

High reverse breakdown voltage Schottky rectifiers without edge termination on Ga$_2$O$_3$
Applied Physics Letters **110**, 192101 (2017); https://doi.org/10.1063/1.4983203

Perspective: Ga$_2$O$_3$ for ultra-high power rectifiers and MOSFETS

S. J. Pearton,[1,a)] Fan Ren,[2] Marko Tadjer,[3] and Jihyun Kim[4,a)]

[1]*Department of Materials Science and Engineering, University of Florida, Gainesville, Florida 32611, USA*
[2]*Department of Chemical Engineering, University of Florida, Gainesville, Florida 32611, USA*
[3]*U.S. Naval Research Laboratory, Washington, DC 20375, USA*
[4]*Department of Chemical and Biological Engineering, Korea University, Seoul 02841, South Korea*

Gallium oxide (Ga$_2$O$_3$) is emerging as a viable candidate for certain classes of power electronics with capabilities beyond existing technologies due to its large bandgap, controllable doping, and the availability of large diameter, relatively inexpensive substrates. These applications include power conditioning systems, including pulsed power for avionics and electric ships, solid-state drivers for heavy electric motors, and advanced power management and control electronics. Wide bandgap (WBG) power devices offer potential savings in both energy and cost. However, converters powered by WBG devices require innovation at all levels, entailing changes to system design, circuit architecture, qualification metrics, and even market models. The performance of high voltage rectifiers and enhancement-mode metal-oxide field effect transistors benefits from the larger critical electric field of β-Ga$_2$O$_3$ relative to either SiC or GaN. Reverse breakdown voltages of over 2 kV for β-Ga$_2$O$_3$ have been reported, either with or without edge termination and over 3 kV for a lateral field-plated Ga$_2$O$_3$ Schottky diode on sapphire. The metal-oxide-semiconductor field-effect transistors fabricated on Ga$_2$O$_3$ to date have predominantly been depletion (d-mode) devices, with a few demonstrations of enhancement (e-mode) operation. While these results are promising, what are the limitations of this technology and what needs to occur for it to play a role alongside the more mature SiC and GaN power device technologies? The low thermal conductivity might be mitigated by transferring devices to another substrate or thinning down the substrate and using a heatsink as well as top-side heat extraction. We give a perspective on the materials' properties and physics of transport, thermal conduction, doping capabilities, and device design that summarizes the current limitations and future areas of development. A key requirement is continued interest from military electronics development agencies. The history of the power electronics device field has shown that new technologies appear roughly every 10-12 years, with a cycle of performance evolution and optimization. The older technologies, however, survive long into the marketplace, for various reasons. Ga$_2$O$_3$ may supplement SiC and GaN, but is not expected to replace them. *Published by AIP Publishing.*
https://doi.org/10.1063/1.5062841

INTRODUCTION

There is interest in a number of less developed semiconductors with bandgaps larger than GaN or SiC[1–13] for power switching and power amplifier applications.[2,13,14] The discrete power device market cap is estimated to be between $15 and $22 and is comprised primarily of transistors and diodes in a variety of voltage, current, packaging, and power ratings. It is an area of intense focus as new technologies, such as wide bandgap (WBG) semiconductors, and new applications, such as electric vehicles and lightweight systems like drones, emerge. These materials include diamond,[15–21] BN,[22] high Al-AlGaN,[23–27] and Ga$_2$O$_3$.[28–33] While the initial device performance on these so-called ultra-wide bandgap (UWB) semiconductors looks promising, many challenges exist, including growth maturity, thermal limits, cost, and reliability in these material systems.[13,14,18,25,29] Both SiC and GaN devices have made enormous progress in power switching

and/or power amplifier applications.[1–13] Beyond the recognized markets in power control and switching applications, lidar sensors for autonomous vehicles, multi-level converters, and motion control for robotics are emerging areas. These expanded markets for SiC and GaN devices have their own unique requirements for performance and design. There is interest in extending the performance limits using other semiconductors that could potentially outperform SiC/GaN technology.[2,13,14,25,28,29] One thing that history teaches us in this area is that it will take decades of development across growth, processing, and device design platforms for this to occur. For example, it took ∼35 years from conception to commercialization for SiC power devices.[1,5,6] Who will bear the cost of this development? Without an established revenue stream to support R&D over such a long time span, the clear driver has to be high-payoff military applications so that the necessary funding is there for long enough to truly develop this into a mature, manufacturable technology. It has never been the case with compound semiconductor power electronics that commercial applications have initially driven and sustained the development. GaAs went through an extended adolescence because of its promise for military

a)Authors to whom correspondence should be addressed: spear@mse.ufl.edu and hyunhyun7@korea.ac.kr

radar and microwave communications before maturing and being used in cell phone chips.[34–38] GaN electronics clearly benefited from the push for green/blue LEDs and laser diodes and the advances in growth and processing made in the photonics arena. However, military funding proved crucial for GaN electronics, where they are now employed in active electronically scanned arrays for radar, electronic warfare, and communications systems, but the commercial spinoffs to base stations in 5G communication systems are still emerging.[39–44] Commercial GaN radio frequency (rf) transistors appeared in 2004, with 100 V devices in 2008 and 600 V devices in 2012. SiC was touted for power flow control systems for decades before the technology matured and this long period of gestation was largely the result of military-based funding.[1,5] In forecasting the potential applications of new technologies like Ga_2O_3, there are numerous factors to consider, including production capacity and wafer sizes, substrate availability and manufacturability, second sourcing options, cost, and device performance.

For the purposes of this paper, we exclude diamond, based on cost, and AlN and BN, based on immaturity of growth and doping, although there is a commercial vendor for AlN substrates. The high-Al AlGaN technology looks highly suited to lateral power devices but lack of large area, cheap native substrates, and issues with vertical conductivity may limit its use in vertical power devices.[23–27] In addition to having a lower electron mobility than binary alloys, high Al-AlGaN is difficult to dope controllably and selectively. The usual Si dopant ionization level becomes very deep in Al-rich AlGaN, and ion implantation activation efficiency is low. We will focus on whether Ga_2O_3 has a role in complementing SiC and GaN. Some of the key issues include the real application space of UWB semiconductors in power switching or RF power amplification, whether in realistic conditions they are capable of outperforming the mature SiC and GaN technology, and whether the material quality and cost, thermal problems, and reliability challenges will limit their application. The biggest difficulties in implementing Ga_2O_3 relate to its high thermal resistance and the absence of p-type conductivity through doping with acceptors. This limits the type of device structures that can be realized and requires effective thermal management approaches. We discuss some potential solutions to these issues later in the article.

PROPERTIES AND APPLICATIONS OF Ga_2O_3

The β-phase of Ga_2O_3 has a large bandgap (4.8 eV), breakdown field (6-8 MV/cm), reasonable electron mobility, and availability of native single crystal substrates using inexpensive melt-based growth methods.[45–58] These properties hold promise for improvements in the size, weight, and power (SWaP), as well as the cost of a broad range of power switching and RF components used in power supply, radar, electronic warfare, and communication systems.[13,14] Table I gives a comparison of properties of the main wide bandgap semiconductors.[13,14,17,22,25] Commercially available SiC and GaN power devices still have a high cost and limited availability of the native substrates compared to Si. SiC and GaN

cannot be grown from the melt like Si and the commercialized techniques for their growth, such as seeded sublimation (also known as physical vapor transport, PVT), ammonothermal, and hydride vapor phase epitaxy (HVPE), only produce relatively high cost substrates in limited sizes.[59,60] By contrast, for Ga_2O_3, the bulk growth methods of Czochralski, float-zone (FZ), edge-defined film-fed growth (EFG), and vertical Bridgman methods all produce low cost, large crystals.[58–63] The properties can be related to potential applications through the representation in Fig. 1, which shows that Ga_2O_3 is best suited to high voltage applications because of its large bandgap. Combining Ga_2O_3 with In_2O_3 or Al_2O_3 allows tuning of the atomic and electronic structure.

The maximum voltage that a semiconductor device can sustain is limited by the on-set of avalanche breakdown created by the impact ionization process.[64–73] This is characterized by the impact ionization coefficients for electrons and holes, which are defined as the number of electron-hole pairs created by the mobile particle traversing 1 cm through the depletion region along the direction of the electric field.[72,73] The measurement of these coefficients is complicated by the presence of defects in the semiconductor material, non-uniform electric fields within the structure, and the onset of premature breakdown at the edges of the chips.[66,67,69–71] Another issue in particular applications is thermal management. For example, GaN RF devices may be operated at extreme, highly-localized power densities ($\sim 10^5$ W cm^{-2}), exceeding that of the surface of the sun ($\sim 10^3$ W cm^{-2});[74–85] the RF community needed improved thermal management to fully enable GaN's electronic capabilities.[74–85] GaN high electron mobility transistors (HEMTs) are capable of much higher switching speeds than Si MOSFETs. The faster switching speeds also magnify the impact of parasitic inductances on performance. As GaN matures and becomes capable of even higher switching speeds, the minimization of parasitics will be even more critical to fully utilizing GaN transistors. Even though the carrier mobility in bulk Ga_2O_3 is inherently lower than the other materials, it does not hamper its usefulness for power applications, since the FOM is more dependent on the breakdown electric field than the mobility (cubic dependence of the breakdown field vs linear dependence of mobility).

Finally, existing Si, SiC (vertical devices), and heteroepitaxial GaN (lateral devices) enjoy tremendous advantages in terms of process maturity, an advantage that is especially true for Si, where the ability to precisely process the material has resulted in devices such as super-junctions that surpass the unipolar "limit."[1,2,4,6,9] Despite these challenges, a compelling case can nonetheless be made for the investigation of ultra wide bandgap (UWBG) materials. Tamura Corporation, Novel Crystal Technology (NCT) (for epilayers), Leibniz Institute for Crystal Growth Berlin (IKZ), and more recently Synoptics, a division of Northrop Grumman, have demonstrated all or some of the various orientations, namely (2– 01), (010), and (100), β-Ga_2O_3 bulk substrates in different sizes with on and off-axis orientations. Figure 2 shows photographs of bulk ingots grown by different methods.[63] There are aggressive plans in place to reduce the cost of the resulting wafers to be comparable to sapphire substrates of the same size.[86] It is worth noting

TABLE I. Comparison of properties of SiC and GaN with potential wide bandgap semiconductors for power electronics. GaN data from R. Eden, SiC and GaN Power Semiconductors Report—2016 (IHS), Silicon Carbide & Gallium Nitride Power Semiconductors, see https://technology.ihs.com/521146/sic-gan-power-semiconductors-2016.[263] Diamond data from U.S. Department of Energy, in *Quadrennial Technology Review 2016* (2015), see http://energy.gov/sites/prod/files/2015/09/f26/QTR2015-06-Manufacturing.pdf.[264] Geological Survey, Report on Diamond (Industrial) (2016). Retrieved from http://minerals.usgs.gov/minerals/pubs/commodity/diamond/mcs-2016-diamo.pdf.[265]

Parameter	SiC	GaN	High-Al AlGaN	Ga_2O_3	Diamond	Advantages of Ga_2O_3	Disadvantages of Ga_2O_3
Bandgap (eV)	3.3	3.4	5.8 ($Al_{0.7}Ga_{0.3}$)-6.2 (AlN)	4.85	5.5	Larger means higher critical breakdown field	
Critical Breakdown field ($MV cm^{-1}$)	2.6	3.3	12.7 ($Al_{0.7}Ga_{0.3}$)-16 (AlN)	5-9	10	Larger than SiC or GaN-values have reached ~0.5 the theoretical max	Lower switching speed
Electron Mobility	1000	1200	310	250	2000		Absence of pn junctions
Hole Mobility	90–120	120	~30	N/A	450		
Thermal cond (W m^{-1} K^{-1})	370	130	320	10-30	2000		Low and anisotropic
Impact ionization coefficients	$\alpha = 2.78 \times 10^6$ exp $(-1.05 \times 10^7/E)^{137}$ cm^{-1} $\beta = 3.51 \times 10^6$ exp $(-1.0 \times 10^7/E)^{109}$ cm^{-1}	$\alpha = 5 \times 10^8$ exp $(-3.4 \times 10^7/E)$, $\beta = 6.8 \times 10^6$ exp$(-1.9 \times 10^7/E)$	Not measured	$\alpha = a.$exp $(-b/E)$, $a = 2.5 \times 10^6$ cm^{-1}, $b = 4 \times 10^7$ V cm^{-1}	$a_n = 1.89 \times 10^5$, $a_p = 5.48 \times 10^6$, $b_n = 1.7 \times 10^7$, $b_p = 1.4 \times 10^7$	Comparable to other wide bandgap materials	
Substrate size (in.)	8	8 on foreign substrates-Native substrates still under development (~2 in. diameter)	3–4 on foreign substrates, 2 on AlN	6	1.5(larger on Si)	Competitive with SiC and expected to go lower	
Substrate cost/cm^2 [a]	~8.5	0.2-0.5 on Si, ~110 native substrate	~110 on native GaN substrate	~215	~2.15×10^5 large single crystal	Prices dropping rapidly	
Dopability	Good for both conductivity types	High ionization energies for acceptors	High ionization energies for acceptors	n-type from insulating to 10^{20} cm^{-3}; no p-type doping capability	n-type difficult due to large ionization energy of P		Absence of pn junctions
MOS technology	Yes, nitric oxide anneal	Developmental	Developmental	Primitive	Developmental		Limited gate swing and thermal stability
BFOM	340	870	11773	2870	24660		Suited to high voltage apps
High Temperature Figure of Merit (HTFOM)	0.36	0.10	0.86	0.01	0.06	R_{on} in vertical drift region	Major heat removal issues

[a]SiC data from K. Horowitz, T. Remo, and S. Reese, "A manufacturing cost and supply chain analysis of sic power electronics applicable to medium-voltage motor drives," National Renewable Energy Laboratory, Technical Report NREL/TP-6A20-67694, March 2017 see https://www.nrel.gov/docs/fy17osti/67694.pdf.
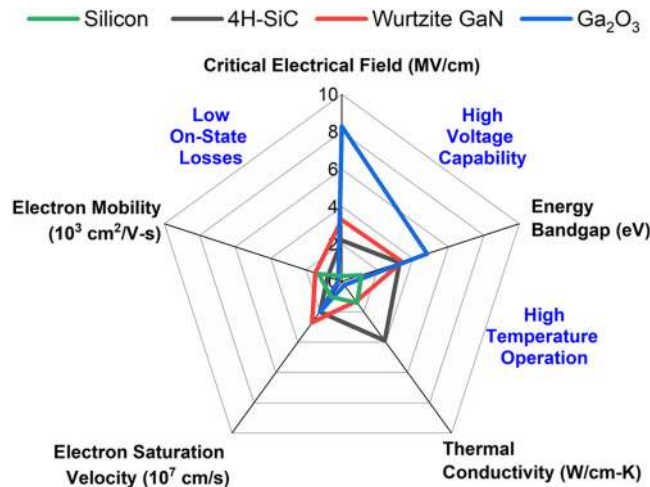
FIG. 1. The pentagon diagram showing the critical material properties important to power semiconductor devices. A larger pentagon is preferred. The data are taken from Refs. 6, 7, and 10.

FIG. 3. Cost comparison of large diameter diamond and Ga_2O_3 crystals (diamond image of the Lesedi La Rona diamond, found in Botswana in 2015. Credit: Donald Bowers/Getty Images North America/Getty Images for Sotheby's). The composite figure is courtesy of Dr. Karl Hobart, Naval Research Laboratory.

that the availability of large, inexpensive substrates is a tremendous advantage for Ga_2O_3, since there are few comparable cases with other semiconductors (Si, GaAs among them). As an example, Fig. 3 shows the cost differential of 3 orders of magnitude between comparable size diamond and Ga_2O_3 crystals.

Another key point from Table I is that there has been no report on p-type doping using acceptor dopants and effective hole conduction in Ga_2O_3 beyond what appears to be conduction at high temperature from native defects expected to be the Ga vacancy.[87–101] Furthermore, self-trapping of holes in bulk Ga_2O_3, which decreases effective p-type conductivity owing to the resultant low mobility, is expected from the first-principles calculation of the Ga_2O_3 band structure.[88,91–94] Theory indicates that all the acceptor dopants result in deep acceptor levels, which were not able to produce p-type conductivity.[87,88]

In terms of commercially available materials, Tamura Corporation provides bulk samples and its recent spinoff, NCT, has also commercialized Ga_2O_3 epilayers grown by molecular beam epitaxy (MBE) and halide vapor phase epitaxy
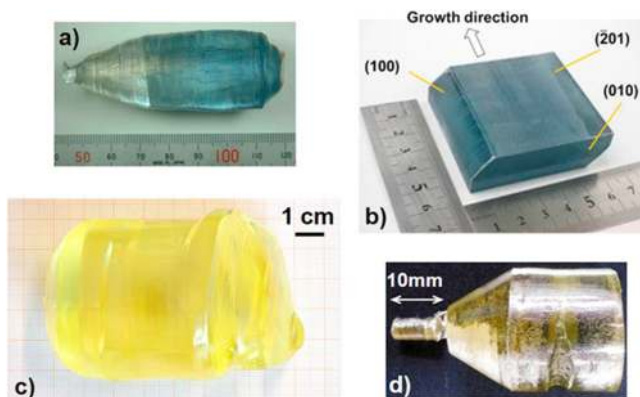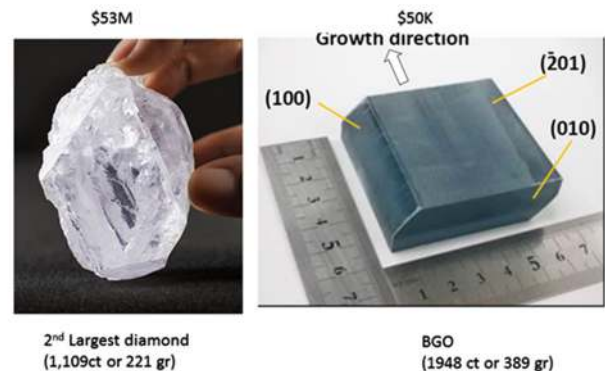

FIG. 2. Bulk β-Ga_2O_3 crystals obtained from the melt by the following methods: (a) Optical Float Zone, (b) Edge Fed Defined Growth, (c) Czochralski, and (d) Vertical Bridgman. Reprinted with permission from Baldini *et al.*, Mater. Sci. Semicond. Process. (in press). Copyright 2018 Elsevier (Ref. 49).

(HVPE). Synoptics is sampling small diameter Fe-doped bulk wafers. Similarly, the only commercial Ga_2O_3 device at present is the Schottky barrier diode offered by Flosfia, Inc. (a spinoff from Kyoto University) and is available in engineering quantities. These devices are fabricated using α-Ga_2O_3 grown by spray-assisted mist-CVD, using a simple precursor of gallium acetylacetonate dissolved in water and transferred as mist particles by a carrier gas to the heated substrate.

The maturity of the technologies is clearly different because of the longevity of SiC and GaN research and development. Forecasts for the SiC power device market are in excess of US$1.4 billion by 2023 with an expected compound annual growth rate (CAGR) near 30% between 2017 and 2023.[5] The main markets are inverters in electric vehicles and their on-board and DC-to-DC converters charging infrastructure, power flow correction power supplies, photovoltaics, uninterruptible power supplies, motor drives, wind, and rail. The SiC market is still being driven by diodes used in power factor correction (PFC) and photovoltaic PV applications, but use of MOSFETs in automotive applications is rising. A typical on-board battery charger application for electric vehicles consists of a power factor correction (PFC) stage and a DC-to-DC converter stage, and both require the highest efficiency possible to deliver as much power as possible to the battery pack. A 3 phase 10 kW PFC based on SiC MOSFET which regulates the output voltage to 700 V starting from a nominal input voltage of 230 Vrms at 50 Hz is needed. Three parameters measure the performances of the system: total harmonic distortion, power factor, and efficiency. Ideally they should be 0%, 1%, and 100% respectively. The Tesla Model 3 is an example of early adoption and is composed of 24 1-in-1 power modules, each containing two SiC MOSFETs thermally dissipated by copper baseplates and a pin-fin heatsink.

In general, system manufacturers are interested in implementing cost effective systems which are reliable, without any technology choice, either silicon or SiC. GaN is moving along the same trajectory for lower voltage applications. The silicon
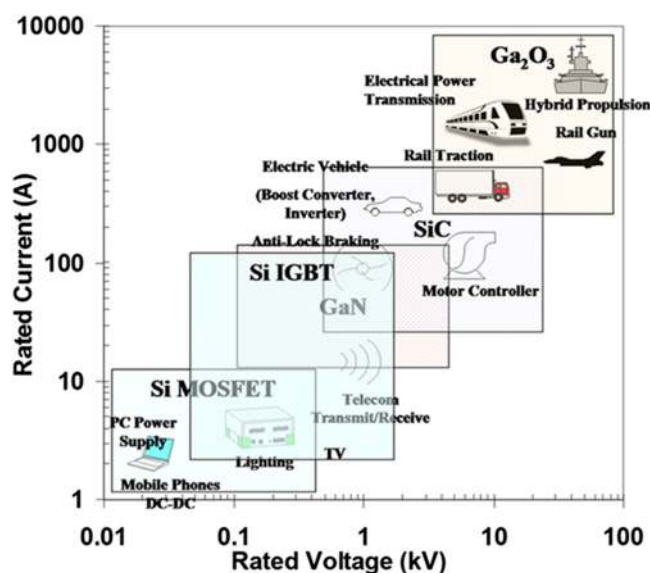
FIG. 4. Applications for Si, SiC, GaN, and Ga_2O_3 power electronics in terms of current and voltage requirements.

power MOSFET journey, spanning more than 30 years, taught us that there are four key variables controlling the adoption rate of a disruptive power management technology.

(1) Does it enable significant new capabilities?
(2) Is it easy to use?
(3) Is it cost effective to the user?
(4) Is it reliable?

The initial thrust on Ga_2O_3 electronics is targeted toward high power converters for both DC/DC and DC/AC
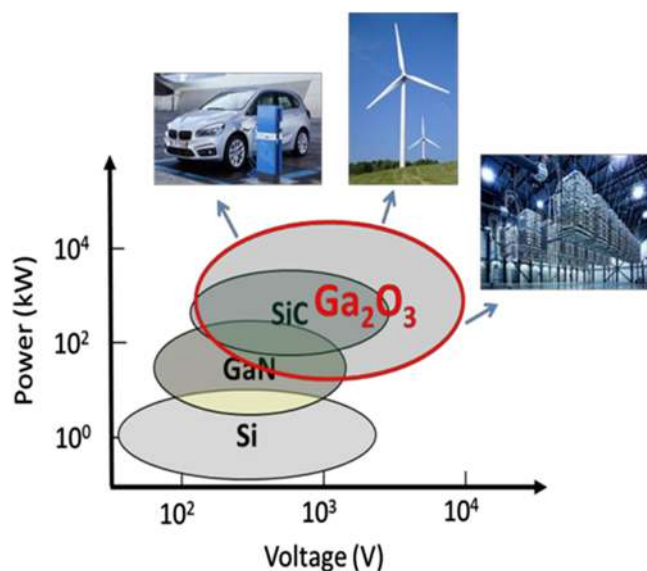

FIG. 5. Additional possible applications for Ga_2O_3 include fast chargers for electric vehicles, high voltage direct current (HVDC) for data centers, and alternative energy sources. These are used to interconnect separate power systems, where traditional AC connections cannot be used. In an HVDC system, electric power is taken from one point in a three-phase AC network, converted to DC in a converter station, transmitted to the receiving point by an overhead line or cable, and then converted back to AC in another converter station and injected into the receiving AC network.

applications.[13,14,29,32] Ga_2O_3 Schottky diodes could supplement 600 V Si or SiC rectifiers targeted at switch mode power converters.[5,43,44] For power switching applications, the operating voltage is limited by the breakdown electric field strength (E_{br}) and the background doping in epitaxial drift layers.[66–70] The total energy loss is determined by resistive power dissipation during on-state current conduction and the capacitive loss during dynamic switching. The power frequency product for Ga_2O_3 is comparable to that for GaN, even though the saturation electron velocity in Ga_2O_3 is lower.[13,14,28] The difference is compensated by the higher E_{br} of Ga_2O_3. Figure 4 shows some suggested application spaces for Ga_2O_3 to take advantage of its large breakdown capability. Figure 5 also shows that Ga_2O_3 could have applications in very high power defense and transportation systems. As discussed earlier, it is likely that defense applications will ultimately decide the commercial success of Ga_2O_3 because of the need for sustained funding to support development of the growth and device technology.

Some of the potential commercial or infrastructure applications for Ga_2O_3 are listed in Table II. The basic device classes delineated for SiC and GaN fall into 3 main groups:[2] 300-1200 V, 5-100 A; 500-1200 V at currents up to 500 A; and finally, 1-6.5 kV with 0.5-8 kA of current rating. The potential replacement of these materials with Ga_2O_3 is hampered by the low thermal conductivity and absence of p-type doping, so that only majority carrier switches are possible unless hybrid oxide p-n heterojunctions are developed. HVDC (high voltage direct current) is used to transmit electricity over long distances by overhead transmission lines or submarine cables. This approach can also be used to interconnect separate power systems, where traditional AC connections cannot be used. In an HVDC system, electric power is taken from one point in a three-phase AC network, converted to DC in a converter station, transmitted to the receiving point by an overhead line or cable, and then converted back to AC in another converter station and injected into the receiving AC network.[1,5–7] Typically, an HVDC transmission has a rated power of more than 100 MW and many are in the 1000–3000 MW range. With an HVDC system, the power flow can be controlled rapidly and accurately in terms of both power level and direction. This possibility is often used to improve the performance and efficiency of the connected AC networks. The most common reasons for selecting HVDC instead of AC include lower investment cost, lower losses, synchronous interconnections, controllability, limited short-circuit currents, environment. Environmental aspects of increasingly important-HVDC has the advantage of lower environmental impact since the transmission lines are smaller and need less space for the same power capacity. One important difference between HVDC and AC is the possibility to accurately control the active power transmitted on a HVDC line. This is in contrast to AC lines, where the power flow cannot be controlled in the same direct way. In the absence of p-doping capability, Ga_2O_3 will be at a fundamental technological disadvantage in the contest for the very high voltage power device market and likely will have limited applicability to these types of systems. It will be better suited to the lower power applications in classification schemes I and II of Table II.

TABLE II. Voltage and current ranges for high power electronics applications, comparing current Si technology with possible replacements and enhancements from the wide bandgap technologies based on SiC, GaN or Ga_2O_3. Adapted from Paul Chow *et al.*, IEEE Trans. Electron Dev. **64**, 856 (2017). Copyright 2017 IEEE.

Classification type	Application	Voltage (V) and current (A) range	Si device type	SiC, GaN, or possible Ga_2O_3 device type
1	Electric vehicle charger	600-1200 V/5-100 A	MOSFET/IGBT	MOSFET, HEMT, rectifier
2	Appliances (AC, induction cookers)	600 V/5-10 A	IGBT	MOSFET, HEMT, rectifier
2	Data center HVDC	800-1200 V/25-250 A	MOSFET/IGBT	Vertical MOSFET, rectifier
2	Electric vehicle power train	500-1000 V/100-500 A	IGBT	Vertical MOSFET, rectifier
3	Photovoltaic inverters, wind farms	1-6.5 kV/0.5-2.5 kA	IGBT	Vertical MOSFET, rectifier
3	AC Drives/Traction	2.5-6.6 kV/0.5-8 kA	GTO thyristor	GaN or SiC IGBT

EPI GROWTH

Thin films of Ga_2O_3 have been grown by evaporation, sol–gel, chemical solution deposition, atomic layer deposition, spray pyrolysis, mist CVD, radio frequency (RF) sputtering, pulsed laser deposition, molecular beam epitaxy (MBE), hydride vapor phase epitaxy (HVPE), and metal organic chemical vapor deposition (MOCVD).[30,32,52,62,102–117] HVPE is capable of growing very thick films at rates of $\sim$10 μm h^{-1}, but the morphology is poor and requires post-growth CMP to planarize. The growth rate for MBE and ALD remains low (0.05-0.1 μm h^{-1}), while MOCVD shows promise of high quality material and practical growth rates (1-3 μm h^{-1}).[115–119] The growth temperatures in the latter case are typically in the range 500-900 °C, which limits diffusion of dopants and mitigates surface dissociation. The typical precursors for Ga are triethylgallium (TEG) and trimethylgallium (TMG), with O_2O_3 or H_2O as the oxygen precursors. A hybrid of MOCVD and HVPE, called Hydride Organometallic Vapor Phase Epitaxy (HOVPE), in a chlorine source is used with a metalorganic to achieve an accelerated growth rate.[30,118] There are no obvious limitations to establishing high quality epitaxial growth technology for Ga_2O_3, since the same techniques established for GaN and GaAs will also work. It is a question of spending the time and effort to optimize these for Ga_2O_3. Agnitron's close-coupled showerhead MOCVD reactor designed to minimize gas phase nucleation of suboxides is a clear step in the right direction.[115]

What are the requirements for devices in terms of directions for epitaxial growth? To make vertical rectifiers, thick drift regions with low background doping are needed. As an example, to achieve 10 000 V breakdown voltage requires 20 μm of Ga_2O_3 with doping <10^{16} cm^{-3}, grown with low defect density on highly conducting substrates. Since the device areas would need to be large (of order 1 cm^2) to carry large currents, the defect density must be low to avoid premature breakdown issues. The growth of ternary alloys involving Al and In (β-(In,Ga)$_2$O$_3$ and β-(Al,Ga)$_2$O$_3$) are needed for modulation-doped transistors, in which the β-(Al,Ga)$_2$O$_3$ bandgap can be tuned from 4.7 eV to above 6 eV.

β-PHASE VERSUS α-PHASE

Corundum α-Ga_2O_3 is the second most studied polytype behind the β-phase because of its simpler epitaxial relationship with *c*-plane sapphire, leading to ease of heteroepitaxial growth on sapphire substrates.[14,29,30,118,120–123] α-Ga_2O_3 is the closest lattice-matched polymorph and has the same corundum structure of sapphire. This metastable, corundum-like α-phase also has potential in the integration of transparent conductive oxide technology with other corundum structure functional oxides, such as Cr, Fe, and V oxides. The potential of alloying with a-Fe_2O_3 and a-Cr_2O_3 opens the possibility of using multiferroic and magnetoelectric effects. The rhombohedral α- (and also the metastable hexagonal ε-Ga_2O_3) phase grows epitaxially on oriented substrates. Moreover, given their similar structures to other wide bandgap materials such as ZnO and AlN, it should be possible to produce functional heterostructures or tunable bandgaps through alloying. The α-Ga_2O_3 has a moderate in-plane a-lattice parameter misfit. All other polymorphs are metastable and transform to the β form at sufficiently high temperatures—this means that in practice only the beta form of Ga_2O_3 can be grown from the melt. For practical applications, it is expected that only the β-polytype will have a significant role. However, the alpha phase does have numerous advantages. For example, α-Ga_2O_3 with the corundum structure has a bandgap of 5.3 eV, with the same structure as sapphire. In addition, alloys that include α-Al_2O_3 (sapphire) and α-In_2O_3 enable bandgap engineering from 3.7 to 8.7 eV.

DEFECTS AND DOPING LIMITATIONS

Considerable effort was expended over a long period to understand the role of the dominant defects in other compound semiconductors, such as EL2 in semi-insulating GaAs, DX centers in AlGaAs, and compensating defects in GaN. The light-mass elements such as H, Li, B, C, N, O, and Si are among the most common elements in nature and are, therefore, the most common contaminants that are introduced into semiconductors during crystal growth and device processing.[124–133] Amphoteric species like Si in GaAs at concentrations of less than 10^{18} cm^{-3} occupies a Ga site (Si$_{Ga}$), where it acts as a donor. At higher concentrations or in Ga-rich material, Si can occupy an As site (Si$_{As}$), where it acts as an acceptor.

P-type conduction by dopants in Ga_2O_3 is predicted to be impossible due to the presence of self-trapping of holes and large effective hole mass. However, for intentional n-type doping, Si, Ge, and Sn appear to be effective-mass like shallow donors without any peculiarity such as DX behavior. Formation of dopant-defect pairs and complexes may reduce the net doping above threshold dopant concentrations. Compensation of shallow donors by Ga$_v$,
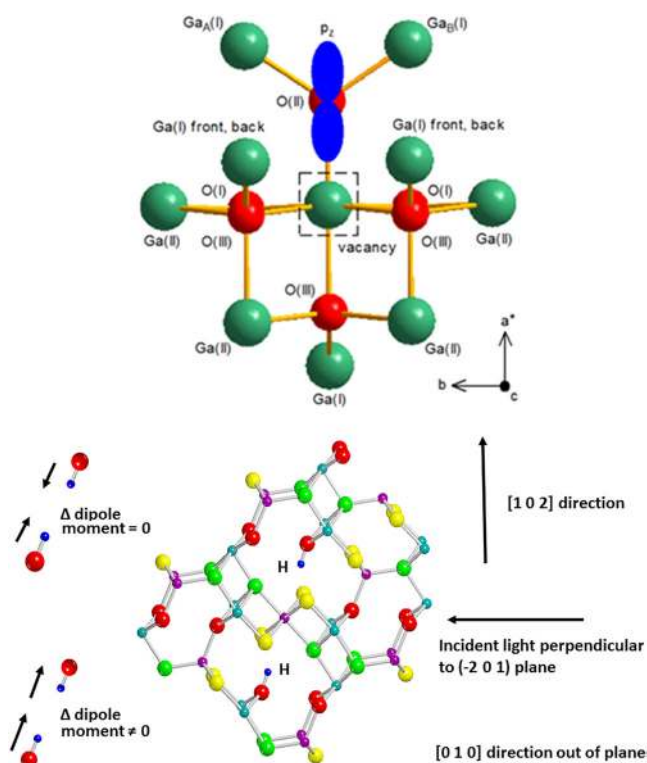
FIG. 6. (Top) Model of the doubly ionized gallium vacancy in β-Ga$_2$O$_3$. An unpaired spin (the hole) is localized in a p_z orbital on a threefold oxygen ion, O(II), adjacent to a gallium vacancy (dashed square) at a sixfold Ga(II) site. Resolved hyperfine interactions are with the two equivalent gallium ions labeled Ga$_A$ (I) and Ga$_B$ (I). Reprinted with permission from Kananen *et al.*, Appl. Phys. Lett. **110**, 202104 (2017). Copyright 2017 AIP Publishing LLC (Ref. 131). (Bottom) Model of V$_{Ga}$-H, the dominant OH center in Ga$_2$O$_3$.

sometimes interacting with hydrogen, may also be present. In bulk crystals grown from the melt, transition metal impurities such as the Ir used in EFG growth may act as compensating acceptors.

Electron paramagnetic and spin resonances (EPR and ESR) have been used to identify shallow donors, acceptors, self-trapped holes, transition-metal ions, and rare-earth ions with unpaired spins. High energy particle irradiation produces a dominant paramagnetic defect with a highly anisotropic g-tensor, superhyperfine interaction with equivalent Ga neighbors and an absence of a central hyperfine interaction with Ga atoms. This is assigned to the V$_{Ga}$ and essentially has the structure of a hole on an oxygen atom adjacent to a cation vacancy. The monoclinic lattice of β-Ga$_2$O$_3$ contains two different Ga sites with tetrahedral and octahedral point symmetry and the assignment of this defect is not ambiguous. Kananen *et al.*[131] also observed singly ionized gallium vacancies (V$_{Ga}^-$) in neutron irradiated β-Ga$_2$O$_3$. The two holes in this acceptor are trapped at individual oxygen ions located on opposite sides of the gallium vacancy and they are weakly coupled and form a triplet S = 1 state. Figure 6 (top) shows their model for the V$_{Ga}^-$ acceptor formed when the V$_{Ga}^-$ acceptor traps a second hole at the O (III) oxygen that is opposite the hole at O(I), the top oxygen ion. The hole is on a threefold oxygen ion at an O (II) site and the gallium vacancy is at the neighboring sixfold Ga(II) site. There has been significant experimental and theoretical examination of the properties of

Ga and O vacancies in Ga$_2$O$_3$ because these are expected to be the most prevalent defects present and will influence the transport properties.[132–139]

The passivation of dopants and defects in semiconductors by hydrogen is well-known and has an impact on semiconductor technology that is widely recognized. In oxide semiconductors, hydrogen has a strong influence on the electrical properties because it can give rise to shallow donors and can passivate deep compensating defects.[126] For example, hydrogen was found to give rise to shallow donors in ZnO.[124,126] The charge carriers in oxide semiconductors can be delocalized or can be self-trapped to form small polarons.[124,129,133] Of particular interest here are polarons that can be spatially localized in the vicinity of impurities in oxides. Hydrogen has been predicted to be an *n*-type dopant in In$_2$O$_3$ that gives rise to unintentional conductivity.[126] Gallium vacancies have low formation energy in Ga$_2$O$_3$, but in the presence of hydrogen, however, the formation energies are reduced and vacancy-hydrogen complexes may form. In β-Ga$_2$O$_3$, annealing intrinsic wafers in atomic hydrogen or deuterium produced dominant hydrogen-induced defect consisting of two hydrogen atoms trapped at a gallium vacancy site (relaxed V$_{Ga}^-$ 2H center), which can act as either a source or a sink for hydrogen.[128] They found the IR vibrational band peak for this defect site at 3437 cm^{-1} The microscopic representation of the center is shown in Fig. 6 (bottom). Annealing in an H$_2$ ambient, followed by rapid cooling, produced a reservoir of hydrogen defects that were not as thermally stable as the V$_{Ga}$-2H center. Some of these are shallow donors that are converted into the VGa-2H defect upon annealing in an inert ambient. More studies of this type, combined with theoretical work, will identify the other main defects and impurities and their effect on electrical properties in Ga$_2$O$_3$. The compensation of donors by F has also been noted in oxides, including Ga$_2$O$_3$.[129,130]

In terms of device requirements, the doping control needs to be from the lowest background n-type concentration possible (i.e., $<10^{16}$ cm^{-3}) to as high as possible for the contacts regions ($>10^{19}$ cm^{-3}). As we discussed earlier, the absence of p-type conductivity due to self-trapped hole formation eliminates the possibility of conventional p-n junctions, although it may be possible to use heterojunction structures involving p-type oxides on Ga$_2$O$_3$. At this stage, that approach has not yielded high quality heterojunctions.

Ga$_2$O$_3$ RECTIFIERS

Schottky rectifiers made on wide bandgap semiconductors have fast switching speed, important for improving the efficiency of inductive motor controllers and power supplies, as well as low forward voltage drop and high temperature operability. Vertical geometry rectifiers fabricated on thick epitaxial layers of β-Ga$_2$O$_3$ on conducting substrates grown by edge-defined film-fed growth (EFG) have shown promising performance in terms of high reverse breakdown voltage (V$_B$ > 1 kV) and low R$_{ON}$, leading to good power figure-of-merits (V$_B^2$/R$_{ON}$).[140–158] Electrical breakdown caused by impact ionization process will preferentially occur at the contact periphery if the maximum electric field in these areas

is not reduced by proper edge termination design.[70,71,159–163] Currently, all Ga$_2$O$_3$ rectifiers show performance limited by the presence of defects and by breakdown initiated in the depletion region near the electrode corners.[140–142,144–148,156–159] In SiC rectifiers, a wide variety of edge termination methods have been employed to smooth out the electric field distribution around the rectifying contact periphery,[9,70] including mesas, high resistivity layers created by ion implantation, field plates, and guard rings. The situation is far less developed for GaO$_3$, with just a few reports of field-plate termination.[142,145,154,156–158,167] The use of edge termination techniques produces a lateral spread of the electric field crowding and depletion layer. This approach is widely used in power device design due to the straightforward inclusion in the fabrication process. There are a number of common edge termination techniques, the most common being field plate edge termination, which uses extension of the Schottky metal over a dielectric layer at the edge to improve the reverse blocking capability. Other approaches such as p-guard rings or junction termination extension are not possible in Ga$_2$O$_3$ due to the lack of p-doping capability and need the use of other p-type oxides integrated into the structure.[164–167]

Reverse breakdown voltages of over 1 kV, with a maximum in the 2.4 kV range, have been reported for β-Ga$_2$O$_3$, even without edge termination.[140–143] The highest reverse breakdown voltages have been achieved with similar layer structures, consisting of a thick epitaxial layer grown on a high quality substrate, approximately 7-20 μm thick lightly Si-doped n-type Ga$_2$O$_3$ grown by HVPE on n$^+$ bulk, (−201) Sn-doped (3.6 × 10^{18} cm^{-3}) single crystal wafers. Diodes

have full area back Ohmic contacts of Ti/Au (20 nm/80 nm), while the Schottky contacts were Ni/Au (20 nm/80 nm) on the epitaxial layers. There may be some pre-treatment of the back surface to enhance conductivity and lower the contact resistance. This may be plasma exposure, ozone cleaning, or ion implantation of donor dopants. A typical device structure is shown at the top of Fig. 7, while the reverse IV is shown at the bottom.

Konishi *et al.*[142] obtained reverse breakdown voltages in excess of 1 kV for diodes employing an SiO$_2$ field plate with 300 nm thickness and length 20 μm. The device structure consisted of 7 μm thick lightly Si-doped n-type Ga$_2$O$_3$ grown by HVPE on n$^+$ bulk, (−201) Sn-doped (3.6 × 10^{18} cm^{-3}) Ga$_2$O$_3$ single crystal wafers. The dislocation density from etch pit observation was approximately 10^3 cm^{-2}. The reverse leakage current was correlated to the dislocation density in (0-10) oriented bulk β-Ga$_2$O$_3$ as revealed upon a hot H$_3$PO$_4$ acid delineation etch for 1 h. The simulated maximum electric field under the anode edge was 5.1 MV/cm, much larger than the theoretical limits for SiC and GaN and similar to the breakdown field for lateral Ga$_2$O$_3$ MOSFETs.[142] Even higher breakdown voltage might be possible by demonstrating a junction barrier Schottky (JBS) diode architecture, where in reverse bias, the drift layer depletes away from the surface by employing a pn junction. In the case of Ga$_2$O$_3$, pn type heterojunctions have been demonstrated using Li-doped NiO$_2$ or Cu$_2$O deposited on Ga$_2$O$_3$ and Ga$_2$O$_3$ deposited on 6H-SiC.[164–167] Another option might be α-(Rh,Ga)$_2$O$_3$.[168] The turn on voltage of pn junction for wide bandgap oxides like Cu$_2$O is higher than Schottky diode. It would be possible to use CuO$_2$ or CuI as the guard ring for Schottky diodes. Note that rectifiers reported to date still show performance well short of theoretical limits, as demonstrated in Fig. 8.

To give an example of breakdown achievable on fairly resistive Ga$_2$O$_3$, current-voltage measurements were performed on O$_2$-annealed MBE Ga$_2$O$_3$ films, producing high (2.47 kV
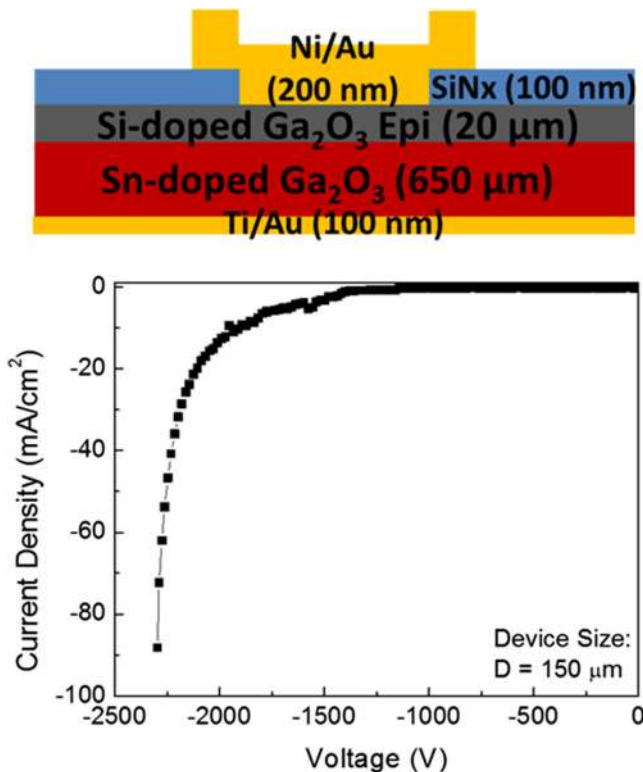

FIG. 7. Schematic cross section of rectifiers with front side Ni/Au rectifying contacts and full area backside Ti/Au Ohmic contacts (top) and reverse I-V characteristic for a 150 μm diameter vertical rectifier diode (bottom).
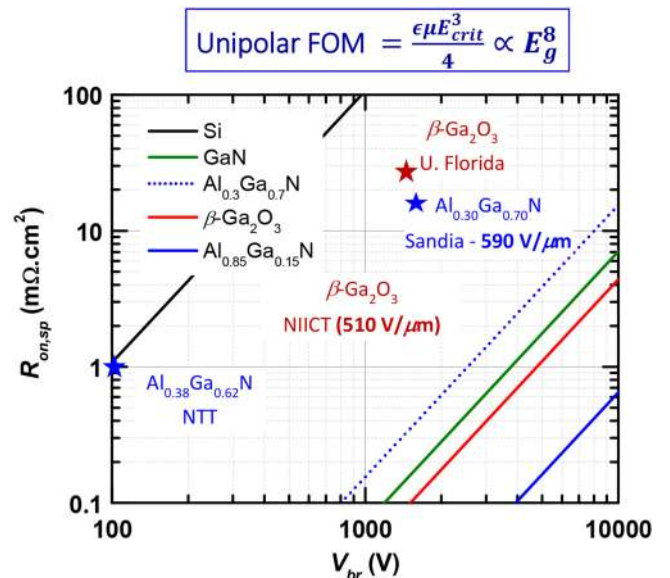

FIG. 8. Plot of on-state resistance for vertical rectifiers on Ga$_2$O$_3$ and AlGaN, along with the theoretical curves for different semiconductors.

for the lateral geometry) reverse breakdown voltage.[155] At low bias, there was minimal current, independent of bias polarity. This high resistivity was not consistent with the carrier concentration measured from the O_2-annealed substrates and could not be explained by passivation of donor states. Secondary ion mass spectrometry indicated significant outdiffusion of Fe from the MBE sample (Fe $\sim 10^{16}$ cm^{-3}). No trace of Fe was detected in as-grown Ga_2O_3 epilayers, even when a Fe-doped substrate was used.

Joishi *et al.*[159] reported field-plate bevel mesa Schottky diodes using LPCVD-grown β-Ga_2O_3 epilayers. The devices had maximum reverse breakdown of 190 V, corresponding to a breakdown field of 4.2 MV cm^{-1}, with an extrinsic R_{ON} of 3.9 mΩ cm^2. Devices without edge termination also show the capability of the Ga_2O_3 to withstand high field strengths.[140,141] The diameter of these contacts ranged from 20 μm to 0.53 mm. The V_{BR} was approximately 1600 V for 20 μm diameter smaller diode and 250 V for 0.53 mm diameter.[140,141] This trend is typical of newer materials' technologies still being optimized in terms of defect density.[39–52] Kasu *et al.*[150,153] examined the effect of crystal defects revealed by etch pit delineation and found that dislocations are closely related to the reverse leakage current in the rectifier and that not all voids produce leakage current. Dislocation defects along the [010] direction were found to act as paths for leakage current, while the Si doping did not affect this dislocation-related leakage current.[148–153] By contrast, in the [102] orientation, three types of etch pits were present, namely a line-shaped etch pattern originating from a void and extending toward the [010] direction, arrow-shaped pits in the [102] direction, and gourd-shaped pits in the [102] direction. Their average densities were estimated to be 5×10^2, 7×10^4, and 9×10^4 cm^{-2}, respectively, but in this orientation there was no correlation between the leakage current in rectifiers and these crystalline defects.[148–153] Thus, the orientation of the substrate determines the sensitivity to defect density.

It is also important to demonstrate high forward conduction currents. Pulsed currents up to 2 A were reported by Yang *et al.*[156,158] Forward I-V characteristics of the devices were measured by applying a voltage pulse (0 V–V_F) to the Schottky contact and monitoring the current using a wideband current probe connected to an oscilloscope. Large area (0.2×0.3 and 0.1×0.3 cm^2) devices could be pushed to above 2 A, with a maximum of 2.2 A. Since these were single sweeps, excessive self-heating was not a significant issue and the devices showed no degradation in performance.

It is worth noting that the reverse breakdown exhibits a negative temperature coefficient. This is usually the result of defects that enhance multiplication, leading to reduced breakdown and has been reported previously in the early stage development of SiC and GaN power electronics.[169,170] In those cases, the impact ionization coefficients (α_p) for holes measured near defects were found to be higher than those measured at a non-defective regions.[169] Also, the values measured near defects were found to increase with increasing temperature, in contrast with a defect free diode, where α_p decreased with increasing temperature, clearly indicating that the defects produce the observed negative temperature coefficient of breakdown voltage.

To summarize the situation for rectifiers, the absence of clear demonstrations of p-type doping in Ga_2O_3, which may be a fundamental issue resulting from the band structure, makes it difficult to simultaneously achieve low turn-on voltages and ultra-high breakdown because of the absence of a p-i-n rectifier technology. Devices based on β-Ga_2O_3 have not yet reached the expected 8 MV/cm theoretical value for breakdown voltage. The best Schottky barrier diodes based on β-Ga_2O_3 have achieved a breakdown strength of $\sim$4 MV/cm. Care must be taken to ensure proper and efficient termination of the junction at the edge of the die; if the junction is poorly terminated, the device breakdown voltage can be as low as 10%–20% of the ideal case. Such a severe degradation in breakdown voltage can seriously compromise device design and lead to reduced current rating. The purpose of the various edge termination techniques is to reduce electron-hole avalanche generation by lowering the peak electric field strength along the semiconductor surface and thereby shifting the avalanche breakdown location into the bulk of the device.

The future direction in this area is that large-area and vertical devices will mirror the designs of Si, SiC, and GaN power devices, particularly with an emphasis on vertical design with defined conduction paths, such as the current aperture vertical transistor (CAVET) and the vertical fin-channel junction field-effect transistor (JFET). The relatively low thermal conductivity of Ga_2O_3 creates self-heating effects that must be mitigated in order to utilize it for high-power at even moderate switching frequencies. The question remains as to whether Ga_2O_3 will have significant commercial advantages over the more mature SiC and GaN technology for power switching and power amplifier applications. While the initial device performance looks promising, challenges exist including growth maturity, thermal limits, cost, and device reliability. The continued optimization of material quality, device design, and process technology should lead to significant advances in power performance.

Ga_2O_3 MOSFETS

There are significant challenges for Ga_2O_3 MOSFETs in finding an application space not currently filled by SiC devices. To do so, Ga_2O_3 must offer performance characteristics that are simply not possible using any of these materials. SiC MOSFETs have found application in fast, high-voltage power converters due to the superior system efficiency which can be tracked back to the fundamental properties of SiC: wide bandgap, high critical field, long (μs) minority carrier lifetime, ambipolar doping, among others. GaN heterostructures have been used in the rf space for years and are ubiquitous in cell phone applications, and GaN power transistors are starting to find niche applications in 600 V market segments such as data center server power supplies. What does this reality leave for Ga_2O_3? Mastro *et al.* have suggested that Ga_2O_3 must deliver a tenfold increase in power over SiC, making it a realistic alternative to traveling wave tube (TWT) devices for the low-end of the frequency spectrum.[33] Other niche applications are possible as well. For example, thermal stability of SiC could be sufficient for prolonged operation of spacecraft electronics on Venus, the hottest planet in the

solar system (462 °C).[171,172] However, single event burnout (SEB) due to heavy ion damage is an even bigger problem for SiC MOSFETs in particular, where it has been linked to the parasitic bipolar junction transistor (BJT) formed between source, channel (transistor body), and drain epilayer.[173,174] Since acceptors in Ga_2O_3 are not expected to ionize sufficiently in order to enable controllable p-type doping in this material, it is conceivable to propose that extreme radiation hardness in this material, combined with thermal stability and high power, could offer stable device operation in the most extreme environments known, such as deep space. Furthermore, again due to its ultra-wide bandgap and good radiation tolerance, Ga_2O_3 could also potentially provide a power source for space or underwater electronics if used as a beta-voltaic source, an application which has been particularly well-suited for single crystal diamond.[175] These well-known applications are only an example of what we consider to be the next frontier of electronics: applications where solid-state electronics have never been used before. The journey for Ga_2O_3 is at the very beginning as reports of its fundamental properties such as the anisotropy in bandgap and thermal conductivity, band-to-band transitions, and impact ionization coefficients are just beginning to emerge.[176–179]

Gallium oxide transistor technology has already made remarkable progress and several important milestones in transistor architecture development have been "checked off." In what is perhaps the biggest breakthrough for this material so far, ternary heterostructure field-effect transistors (HFETs) based on an $(Al_xGa_{1-x})_2O_3$ barrier epitaxially grown on a β-Ga_2O_3 buffer on a native substrate have exhibited a two-dimensional electron gas, as evidenced by Shubnikov-de Haas oscillations at low temperature.[180] The lack of p-type doping in Ga_2O_3 means that vertical transistor structures, attractive due to the inexpensive large-area commercial native substrates, have to rely on current channels confined using either implanted current blocking layers or etched fins. Indeed, recent reports of Ga_2O_3 current aperture vertical electron transistor (CAVET) and fin-based vertical junction field-effect transistor (JFET) represent the most promising architectures for Ga_2O_3 device development.[181,182] A key challenge for all Ga_2O_3 devices is to reduce the on-state resistance, defined as Ron = $4BV^2/\varepsilon\mu E_c^3$, where ε is the dielectric constant, μ the carrier mobility, and Ec the critical electric field at the onset of breakdown. The denominator $\varepsilon\mu E_c^3$ is also known as Baliga's figure of merit (BFOM), often used to evaluate the potential improvements in the drift region resistance of unipolar power devices by substituting silicon with other semiconductor materials.

The biggest challenge for oxide HFETs is to demonstrate that they are competitive with nitride technology. Scaled Ga_2O_3 HFETs will be demonstrated in the near future as the large critical field of Ga_2O_3 can support more aggressive device scaling which, combined with the high saturation velocity predicted from theory, can offer new application space for Ga_2O_3 in the radio frequency market.[183] Additional heterostructure engineering at the nanoscale level could also compensate for the lack of polarization engineering in β-Ga_2O_3 as well as the lower room temperature bulk mobility of this material (200-250 $cm^2/V\,s$). For the CAVET, a current

blocking layer (CBL) formed with implantation of N, instead of Mg, has been shown to perform much better[184] and could lead to a high breakdown voltage. For the vertical JFET, integration of an anisotype semiconductor heterojunction instead of an MOS gate could improve blocking capability and reduce off-state current.[185]

Although normally off Ga_2O_3 MOSFETs have been reported by several groups,[186–192] most Ga_2O_3 devices reported to date have mainly been depletion-mode, with undoped or n-type channels and employing SiO_2, HfO_2, or Al_2O_3 dielectrics.[29,190–210] The wide bandgap of Ga_2O_3 means there are limited choices to obtain sufficient band offsets with the dielectric.[211–217] We expect that MOS gate engineering for Ga_2O_3 will be a significantly more challenging problem than it was for SiC. The low mobility of inversion electrons in SiC MOS channels due to severe electron trapping and scattering at the SiO_2/4H-SiC interface has been the main problem for power MOSFETs.[218–222] Unlike Si MOSFETs, post-metallization anneals with H_2 do not reduce these interface traps (or defects), resulting in higher than ideal on-state resistance SiC devices. The introduction of a post-oxidation annealing in nitric oxide (NO) was a huge breakthrough for reducing SiC channel resistance[218] and improving the interface defect density (D_{it}) near the conduction band edge on 6H-SiC. This led to the improvement of channel mobility and reduction in forward conducting resistance. Comparable breakthroughs have not commenced in Ga_2O_3.

The success of two-terminal device commercialization will be essential for future efforts in transistor development. The SiC Schottky diode similarly was commercialized almost a decade before the MOSFET. Both breakdown mechanisms and extended defects in Ga_2O_3 are beginning to be better understood, which inevitably will lead to improvements in device performance.[193,194] Perhaps most importantly, thermal issues in Ga_2O_3 due to its very low thermal conductivity must be addressed. The importance of thermal management is being recognized in the community, and the reports so far indicate that pulsed operation will not be sufficient to avoid significant self-heating in
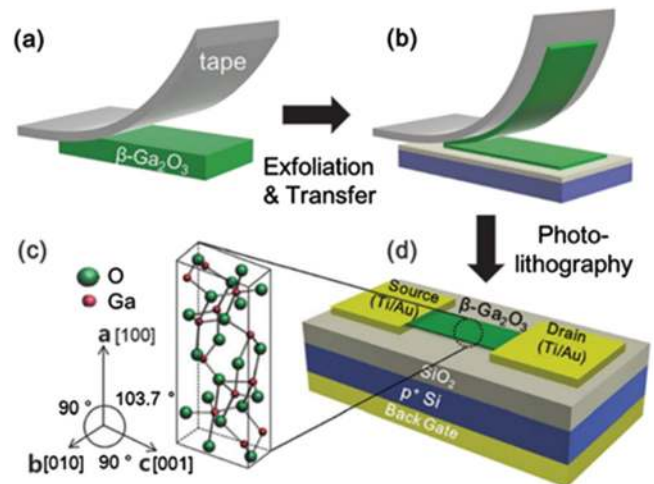

FIG. 9. Schematic of mechanical exfoliation of β-Ga_2O_3 flakes using Scotch-tape method and fabrication of device using the exfoliated flake.

Ga$_2$O$_3$ devices.[195,196] Thermal issues and management are discussed in more detail in a later section.

Ga$_2$O$_3$ FETs AND SOLAR-BLIND PHOTODETECTORS ON EXFOLIATED FLAKES

There have been a large number of reports of photodetectors, diodes, and mosfets fabricated on exfoliated Ga$_2$O$_3$ flakes or membranes.[219–234] A schematic of the process to produce Ga$_2$O$_3$ flake devices is shown in Fig. 9. Ga$_2$O$_3$ is not a van der Waals material, which means that it is not a layered material. However, the huge anisotropy in the lattice constants (a [100] = 12.225 Å and b [010] = 3.039 Å, c [001] = 5.801 Å) of monoclinic β-Ga$_2$O$_3$ allows it to be separated into individual free-standing flakes, which has been called nano-layer, nano-menbrane, or nano-belt. Hwang *et al.* reported that there are two facile cleavage planes along (100) and (001) planes in monoclinic β-Ga$_2$O$_3$ crystal.[229] Unlike graphene and other two-dimensional (2D) transition metal dichalcogenide (TMD) materials, it is challenging to obtain mono-, bi-, or few-layers from β-Ga$_2$O$_3$ crystal because it is not a layered material. Until now, the reported (opto)electronic properties of the exfoliated β-Ga$_2$O$_3$ flakes have not been different from those of the bulk crystal because the exfoliated flakes are still thick. In 2D materials including TMDs and black phosphorus, the thickness-dependent variations of the energy bandgap are well known. Therefore, it is expected that one can engineer (opto)electronic properties of β-Ga$_2$O$_3$ by thinning it down to few layers using (dry or wet) etch and liquid/mechanical exfoliation methods. Kwon *et al.* reported the plasma-assisted thinning of β-Ga$_2$O$_3$ from 300 nm down to ∼60 nm.[231] The merits of the exfoliated Ga$_2$O$_3$ nano-layer include its high crystallinity, no memory effect from the substrate, strain-free, and facile formation of heterostructure using other n-type or p-type semiconductors. For example, the lack of p-type Ga$_2$O$_3$ may be substituted by using p-type diamond, forming p-n heterojunction.

Various electronic devices using the exfoliated β-Ga$_2$O$_3$ flakes have been demonstrated including MOSFET, metal insulator field effect transistor (MISFET), Schottky diode, p-n diode, and junction FET. Since p-type β-Ga$_2$O$_3$ is still not available, heterostructures are necessary to form p-n junctions. Kim *et al.* demonstrated an exfoliated β-Ga$_2$O$_3$ based FET with high on/off ratio, which operated up to 250 °C.[224] Stacked heterostructures of p-Si/n-Ga$_2$O$_3$ and p-WSe$_2$/n-Ga$_2$O$_3$ exhibited typical p-n junction behaviors, confirming the formation of p-n heterojunction. Kim *et al.*[232] reported JFET with long-term stability using p-WSe$_2$/n-Ga$_2$O$_3$, where β-Ga$_2$O$_3$ is an n-type channel layer β-Ga$_2$O$_3$ nano-layer FET with hexagonal-boron nitride field plate exhibited off-state breakdown voltage as high as 344 V, presenting the potential of high power nanoelectronics.[233]

In summary, the ultra-wide bandgap of β-Ga$_2$O$_3$ is ideal for solar-blind photodetectors. Therefore, different nano-optoelectronic devices to detect UV-C wavelengths have been reported using the exfoliated β-Ga$_2$O$_3$ flakes, including photoconductive detector, metal-semiconductor-metal photodetector, and Schottky-barrier photodiode. These devices have exhibited good photo-response characteristics with fast switching, high responsivity, and good UV-C/UV-A rejection ratio. The integration of the exfoliated β-Ga$_2$O$_3$ nano-layer with graphene was especially helpful to improve the photoresponse characteristics because graphene is UV-transparent and conductive electrode.[234] Furthermore, the heterostructures of the exfoliated β-Ga$_2$O$_3$ nano-layer/other 2D materials can open a door to the novel functional devices. Although Ga$_2$O$_3$ is an excellent candidate material for a solar-blind photodetector, the persistent photoconductivity and defect-induced non-idealities which are common in oxide and III-nitrides need to be addressed. Also, the surface defects induced by the mechanical exfoliation seem to limit the (opto)electronic device performances because a lot of dangling bonds are created by the physical separation process. Therefore, appropriate passivation methods by PECVD and ALD or damage removal method by etch process need to be investigated.

THERMAL CONDUCTIVITY

β-Ga$_2$O$_3$ exhibits an anisotropic and low thermal conductivity, with room temperature values for the main crystal axes of λ[100] = 11 ± 1 W/(m K), λ[010] = 29 ± 2 W/(m K), and λ [001] = 21 ± 2 W/(m K).[74–85,235–240] The presence of unintentional defects such as the Ga vacancies discussed earlier significantly degrades the thermal properties.[39,240] Simulations indicate that at 25 °C, 1% and 2% oxygen vacancies decrease the thermal conductivity by 8.5% and 14.3% in [100] direction, 14.9% and 24.1% in [010] direction, 10.7% and 17.4% in [001] direction, respectively.[239,240] Consequently, diamond-based heat spreader technology developed for GaN[241,242] will be needed for Ga$_2$O$_3$. Depending on thickness, grain size, and content of sp^2 bonded carbon in the film, synthetic CVD-grown diamond can have 3 to 4× better thermal conductivity than Cu, whose thermal conductivity is 400 W/m K.[243] For GaN devices, SiC (thermal conductivity up to 400 W/m K) is the most thermally conductive substrate material used commercially, but even this is insufficient at very high powers. As a result, commercial GaN rf devices are typically de-rated to minimize self-heating effects and meet reliability qualification targets. On the other hand, the low dielectric constant of CVD diamond and the commercial availability of large-area polycrystalline diamond substrates makes them an excellent candidate for high frequency/power applications.

Industrial-grade synthetic diamond has thermal conductivity ranging from 1200 to 2000 W/m K. GaN device manufacturers exploit its potential to increase the performance of discrete and Monolithic Microwave Integrated Circuit (MMIC) devices, both as a substrate and as a heat spreader. There are currently a few companies developing GaN-on-Si. In addition, Al-diamond metal-matrix composites (MMC) and Ag-diamond-silver composites consisting of diamond particles in a matrix of silver alloy with thermal conductivity 650 W/m K at room temperature and a CTE close to that of the semiconductors and significantly larger than that of conventional packaging materials such as CuW, are increasingly used as heat spreaders for GaN devices with very high RF output powers.[244,245]

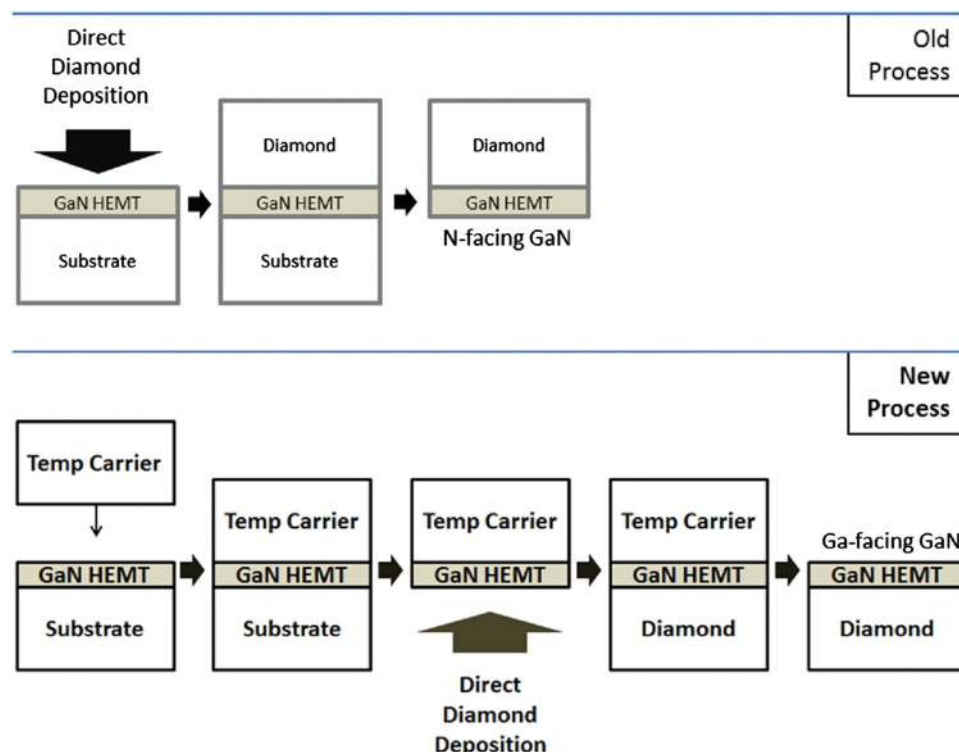In present GaN-on-Diamond devices, a thin barrier dielectric layer is required on the GaN surface to enable

FIG. 10. Schematic of process used for incorporating a diamond heat-sink on GaN HEMTs, which involves thinning or removing the substrate and then depositing diamond on the opposite side.

seeding and successful deposition of diamond onto the GaN. As a result, a significant thermal boundary resistance (TBR) then exists in these devices at the GaN-dielectric-diamond interface, which lowers the overall thermal benefit of this technology. A schematic of the original and more optimized direct diamond deposition process is shown in Fig. 10. Reducing the thickness of the barrier dielectric (typically SiN) can lead to ineffective protection of the GaN surface, especially N-polar GaN. The optimization of the backside process has thus evolved into somewhat an art over the past decade, initially developed at Group4 Labs and subsequently acquired by Element Six.[246] Most likely, the technical details of the successful diamond integration process for Ga_2O_3 will also remain highly proprietary but initial attempts at thermal management of Ga_2O_3 are already being developed. The demonstration of a nanomembrane FET by exfoliating Ga_2O_3 onto single crystal diamond by Noh and coworkers is the first direct attempt at integrating Ga_2O_3 and diamond.[247]

More advanced Ga_2O_3 transistor cooling demonstrations are expected to follow in the near future. A great amount of know-how was developed under several DARPA programs, such as NJTT and ICECool, leading to reductions in device thermal resistance near the junction of the transistor using cooling techniques such as microfluidics. The payoff resulted in a demonstration of a threefold improvement in power density while preserving RF capabilities using substrate-side cooling which allowed gate fingers to be placed much closer together. The improvement was attributed to a 40% reduction in thermal resistance for a GaN-on-Diamond process compared to commercial GaN-on-SiC technology. Raytheon developed etched cooling channels in a diamond substrate and attached it to the thinned wafer, avoiding some of the manufacturability issues with growing the GaN on the diamond substrate, and added liquid cooling. A glycol/water coolant is flowed through

the channels within $100 \, \mu m$ of the active HEMT area. They demonstrated a wideband continuous-wave (CW) amplifier with 3.1× the power output and 4.8× the power density of the baseline amplifier currently designed into a next-generation electronic warfare system. The device change in temperature from the GaN channel to the substrate bottom was found to be reduced by 80 °C when compared to the same device on GaN
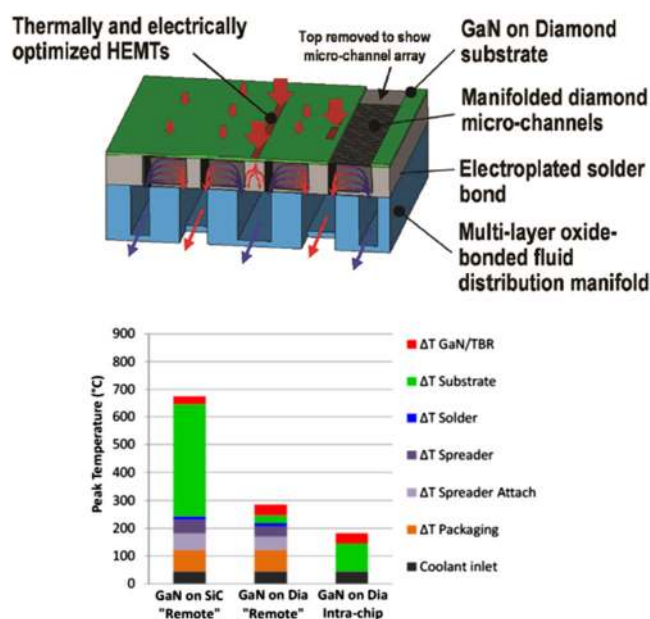

FIG. 11. (Top) Microfluidic intra-chip cooling structure and (bottom) summary of peak temperature rise for GaN-on- SiC and GaN-on-diamond remote cooling and intra-chip diamond microfluidic cooling. From Altman *et al.*, in *ASME 2015 International Technical Conference and Exhibition on Packaging and Integration of Electronic and Photonic Microsystems, San Francisco, California, USA, July 6–9, 2015.* Copyright 2015 ASME. Reprinted with permission from ASME.

on SiC.[82] Most recently, Tadjer and coworkers have directly compared GaN HEMTs before and after the substrate diamond process, showing that the thermal improvement can be even more dramatic.[248]

Monolithic Microwave Integrated Circuits (MMICs) fabricated using GaN on Diamond substrates have the same packaging thermal limitations as GaN on SiC. Therefore, an intra-chip cooling alternative has been developed, eliminating various heat spreaders, heat sinks, and thermal interface layers in favor of integral microfluidic cooling in close proximity to the device junction. This structure employs diamond microfluidics for low thermal resistance die-level heat removal. Through this, MMICs with significantly greater RF output than typical of the current state-of-the-art, dissipating die and HEMT heat fluxes in excess of $1 \, kW/cm^2$ and $30 \, kW/cm^2$, respectively, can be operated with junction temperatures that support reliable operation. A schematic of the structure is shown in Fig. 11.

Fujitsu Laboratories Ltd. developed technology for bonding single-crystal diamond to SiC substrates at 25 °C, to overcome bowing of the wafers due to mismatch of thermal expansion coefficient.[249] Simulations confirmed this would lower thermal resistance by ∼40%.

Pomeroy *et al.*[84] examined the thermal resistance of β-Ga_2O_3 of MOSFETs using Raman thermography and simulation. Single finger β-Ga_2O_3 MOSFETs with a $2 \, \mu m$ gate length ($1 \, \mu m$-long field plate), $200 \, \mu m$ gate width, $5 \, \mu m$ gate-source spacing, and $25 \, \mu m$ gate-drain spacing were studied, having a saturated drain current of 58 mA/mm and a threshold voltage of –30 V, resulting in a simulated peak temperature of 465 °C. The simulated local lateral heat flux through the gate metal was larger than through the Ga_2O_3, suggesting that top-side heat extraction is needed. Replacing SiO_2 with a 200 W/m K diamond thin film reduced the thermal resistance of the investigated device by 30%. Combining thin film heat spreaders with flip chip mounting onto a high thermal conductivity carrier resulted in a significant reduction in thermal resistance.

Lin *et al.*[239] directly bonded Ga_2O_3 to thermally and electrically conductive polycrystalline SiC and demonstrated the formation of a void-free high-quality Ga_2O_3/SiC interface. Another approach is to include rigid heat exchangers on both sides of a power module package.[85]

The main message of this section is to point out that effective thermal management approaches have been developed for GaN and much of that expertise can be applied to Ga_2O_3, where the expected thermal improvements should be even greater.

FUTURE NEEDS

Commercial applications for wide bandgap power electronics include wireless charging, more energy efficient data centers, power flow control in renewable energy systems, more efficient motor drives, and electric vehicles, both in power flow control and recharging systems.[242,244] Since ∼2000, power semiconductors have become increasingly important as the enabler for state-of-the-art consumer applications, industrial systems, and transportation vehicles and automobiles. Several industries have shifted their development

focus gradually toward power semiconductors to provide high-efficiency power conversions and variable motor drives or related systems. According to Yole,[245] electric vehicle/hybrid electric vehicle (EV/HEV) sales will achieve a 28% compound annual growth rate (CAGR) from 2017 to 2023. Start-ups and spin-offs are appearing in the expanding applications opened up by wide bandgap semiconductors and innovative packaging concepts. These approaches serve as the enabler for the new requirements from industry. The very reliable tram and train industry in Japan has started to integrate high-voltage SiC technology and, during the recent Google Little-box challenge, the use of GaN transistors greatly enhanced the power density of a solar inverter. The market for SiC and GaN-on-silicon devices in power electronics is predicted to reach 10% of market share in five years.[245]

The first commercially available SiC diode arrived to market 18 years ago and has progressively replaced Si diodes in some applications. SiC MOSFETs are also commercially available, with improved device reliability and performance. The availability of SiC transistor has enabled realization of full-SiC power modules, providing benefits compared to Si-based power modules. SiC development efforts have been refocused to the manufacturing issues to drive the cost down, technology transfer to 6-in. wafers, improving manufacturing yield, and ramp-up of high volume production.

GaN-on-Si power devices are less mature compared to SiC power devices, but several power device suppliers have entered the mass production phase. The market is driven by low voltage high frequency applications such as Lidar and wireless power, where GaN has its unique selling point, as well as consumer power supply market where the weight and the size are important. For high voltage industrial applications, the reliability issues are still hindering a larger penetration of GaN devices.

For Ga_2O_3 to play a role, its development must be sustained by military funding to apply it in low frequency, high voltage applications beyond the capability of GaN and SiC. It could provide improved efficiency in the critical in the AC-to-DC conversion market. It is unlikely that Ga_2O_3 will displace all other relevant materials in the full range of power and power conversion applications, such as hybrid and electric vehicles, power supplies for computer and telecom and data centers, motor drives, utility and grid control, and wireless power transfer due to the immaturity of the technology. To find an application in the power switching and conversion application space, the following areas need sustained development:

1. **Epitaxial growth**—controlled growth of doped, high quality, homo-, and hetero-epitaxial structures on Ga_2O_3 substrates should be a relatively a straightforward task. It is known from other compound semiconductor growths how to control the background purity and crystal quality using highly refined precursors, buffer layer design, and active layer growth conditions using methods like MOCVD, MBE, and MOMBE. The presence of defects in existing material leads to current collapse in Ga_2O_3 FETs, because the density of traps even in high-quality Ga_2O_3 films is not at all negligible. Similarly, more attention should be paid to

studying the origin of long decay times and even persistent photoconductivity often reported for solar-blind Ga_2O_3 photodetectors, because these effects will seriously hamper practical applications. There is still scope for development of hetero-interfaces for thermodynamically stable oxides such as Al and In.

2. **Improved Ohmic contacts**—use of interfacial engineering and inter-layers such as conducting oxides of Aluminum Zinc Oxide (AZO), ITO, and related materials to reduce specific contact resistance and development of selective ion implantation doping to reduce contact resistance. Ga_2O_3 does not appear to possess a surface electron accumulation layer, unlike In_2O_3, where this layer contributes to the unintentional conductivity and can also be observed as a downward band bending at the In_2O_3 surface.

3. **Thermally stable Schottky contacts**—these might include W and related borides and carbides with high melting temperatures and low reactivity with Ga_2O_3. Deposition by sputtering will need management of near-surface ion damage, and ALD approaches are desirable. It is important to establish if the work function of the metal or surface pinning by defects controls the barrier height. Ga_2O_3-based power device could also benefit from the availability of minority carriers, by integration with p-type oxides so that PIN-diodes and IGBT (insulated gate bipolar transistor) type transistors can be fabricated. These devices preserve the high voltage blocking capacity while lowering on-state resistance, exceeding the theoretical limits of unipolar devices.

4. **E-mode operation**—the absence of p-doping in Ga_2O_3 might be partially addressed by integration with p-type oxides such as CuI,[250–253] Cu_2O,[254] or NiO.[255] GaN-on-Si e-mode devices for 200 V and 650 V applications still are far from optimized, but they have increasingly relied on a p-GaN cap to deplete the channel. Since this is not an option for Ga_2O_3, the technology for Ga_2O_3 normally off devices remains confined to charge balance design as with laterally-depleted finFETs.

5. **Reduction of dynamic R_{ON}**—in both MOSFETs and rectifiers, e.g., rectifiers, when forward biased (on-state) should have minimal voltage across the two terminals and the leakage current should be low when reverse-biased (in the off-state). Schottky diodes have high switching speed but tend to have high leakage in the off-state. Increasing the thickness or decreasing the doping in the drift region increases the breakdown voltage but also increases the on-resistance A higher R_{on-sp} increases conduction loss and lowers switching speed.

6. **Process integration**—SiC is the most advanced WBG semiconductor for power, with main application in the medium to high voltage range (>600 V) followed by GaN with good potential in medium voltage range (<600 V). The success of SiC is partially a result of its generally high compatibility with Si manufacturing technology and Si production lines. However, due to the different physical and chemical properties of SiC, the process steps needed to be changed from standard Si processing. For some process steps, the requirements are so different that they are out of scope for standard Si tools and require special new tools. For instance, for superior thermal gate oxide formation, temperatures up to 1500 °C, along with NO gas annealing capability, are desirable and for dopant activation in SiC, temperatures of ∼2000 °C are needed. GaN technology is also relatively well developed, but issues remain with e-mode approaches and trapping in dielectric/GaN interfaces. The situation for Ga_2O_3 is obviously far less developed and needs a lot of work.

7. **Thermal management through passive and active cooling**—top-side heat extraction will be an effective thermal management strategy for Ga_2O_3. Combining thin film heat spreaders with flip chip mounting of thinned substrates onto a high thermal conductivity carrier will result in a significant reduction in thermal resistance.[256] The existing embedded thermal management approaches developed for GaN by companies like Northrop-Grumman and Raytheon, where cooling is built into the chip, substrate, and/or package to directly cool the heat generation sites using high-thermal-conductivity synthetic diamond material either to line microfluidic channels or to form the substrate of the RF chips, are something that could be quickly applied to Ga_2O_3. Diamond microfluidics-based intra-chip cooling is key to alleviate the thermal impediments of Ga_2O_3.

Performance is generally summarized by the Figure of Merit rating of a technology, while the cost/performance ratio is often compared through specific on-resistance. Many factors, both commercial and technical, govern the choice of the perfect device, and the success of adoption of GaN and SiC devices is both an opportunity and impediment to Ga_2O_3. GaN and SiC currently cover the same voltage ranges, with GaN devices dominating from tens to hundreds of volts and SiC from approximately 1 kV to many kilovolts. Future voltages for GaN devices should range to commercially available 1200 V devices to experimental devices to 3300 V, while SiC devices are now at, and will expand down, to 600 V. In other words, these technologies are largely complementary and will continue to co-exist. Ga_2O_3 will not displace these materials, but possibly supplement them at high voltages. A note of caution is penetration of SiC MOSFETs in electric and hybrid vehicle converters. Some early adopters have already started using SiC, such as Chinese carmaker BYD in its onboard chargers, or US-based Tesla for its Model 3 inverter. Nevertheless, SiC is still used in only small volumes, requiring a back-up solution with silicon IGBTs. Other carmakers are even more conservative and do not see enough system-level benefits to adopt SiC MOSFETs.

What are some possible breakthroughs that would propel Ga_2O_3 into being competitive? High voltage, high mobility $(Al_xGa_{1-x})_2O_3$/GaO scaled transistors which do not suffer from current collapse may be one. Very high power transistors such as >5 kV rectifiers or Ga_2O_3 HFETs on diamond may be another one. At this point, none of the HFETs have been scaled to the point where it can be determined if they will be relevant to rf applications. The initial data on power switching for Ga_2O_3 rectifiers are promising,[257–261] so one possible early market insertion point for Ga_2O_3 would be using rectifiers

made on this material in hybrid systems using Si MOSFETs in power converters. It is crucial to expand the current growth infrastructure to find commercial success.[262] A breakthrough in these areas is needed for this material from today's status quo in order to give it at least one application which will motivate R&D in the years to come.

ACKNOWLEDGMENTS

[1]A. Q. Huang, Proc. IEEE **105**, 2019 (2017).

[2]T. Paul Chow, I. Omura, M. Higashiwaki, H. Kawarada, and V. Pala, IEEE Trans. Electron Dev. **64**, 856 (2017).

[3]J. Millan, P. Godignon, X. Perpina, A. Perez-Tomas, and J. Rebollo, IEEE Trans. Power Electron. **28**, 899 (2013).

[4]A. Merkert, T. Krone, and A. Mertens, IEEE Trans. Power Electron. **29**, 2245 (2014).

[5]J. Wang, V. Veliadis, J. Zhang, Y. Alsmadi, P. R. Wilson, and M. J. Scott, IEEE Power Electron. Mag. **5**, 40 (2018).

[6]G. Liu, B. R. Tuttle, and S. Dhar, Appl. Phys. Rev. **2**, 021307 (2015).

[7]G. R. Chandra Mouli, J. Schijffelen, M. van den Heuvel, M. Kardolus, and P. Bauer, IEEE Trans. Power Electron. **50**, 97–103 (2018), in press.

[8]E. Santi, K. Peng, H. A. Mantooth, and J. L. Hudgins, IEEE Trans. Electron. Dev. **62**, 434 (2015).

[9]A. Q. Huang, Q. Zhu, L. Wang, and L. Zhang, CPSS Trans. Power Electron. Appl. **2**, 118–130 (2017).

[10]B. J. Baliga, Semicond. Sci. Technol. **28**, 074011 (2013).

[11]M. J. Scott, L. Fu, X. Zhang, J. Li, C. Yao, M. Sievers, and J. Wang, Semicond. Sci. Technol. **28**, 074013 (2013).

[12]J. R. Dickerson, A. A. Allerman, B. N. Bryant, A. J. Fischer, M. P. King, M. W. Moseley, A. M. Armstrong, R. J. Kaplar, I. C. Kizilyalli, O. Aktas, and J. J. Wierer, Jr., IEEE Trans. Electron. Dev. **63**, 419 (2016).

[13]J. Y. Tsao, S. Chowdhury, M. A. Hollis, D. Jena, N. M. Johnson, K. A. Jones, R. J. Kaplar, S. Rajan, C. G. Van de Walle, E. Bellotti, C. L. Chua, R. Collazo, M. E. Coltrin, J. A. Cooper, K. R. Evans, S. Graham, T. A. Grotjohn, E. R. Heller, M. Higashiwaki, M. S. Islam, P. W. Juodawlkis, M. A. Khan, A. D. Koehler, J. H. Leach, U. K. Mishra, R. J. Nemanich, R. C. N. Pilawa-Podgurski, J. B. Shealy, Z. Sitar, M. J. Tadjer, A. F. Witulski, M. Wraback, and J. A. Simmons, Adv. Electron. Mater. **4**, 1600501 (2018).

[14]M. Higashiwaki and G. H. Jessen, Appl. Phys. Lett. **112**, 060401 (2018).

[15]J. W. Liu, H. Oosato, M. Y. Liao, and Y. Koide, Appl. Phys. Lett. **110**, 203502 (2017).

[16]H. Kawarada, H. Tsuboi, T. Naruo, T. Yamada, D. Xu, A. Daicho, T. Saito, and A. Hiraiwa, Appl. Phys. Lett. **105**, 013510 (2014).

[17]H. Sato and M. Kasu, Diamond Relat. Mater. **31**, 47 (2013).

[18]C. I. Pakes, J. A. Garrido, and H. Kawarada, MRS Bull. **39**, 542 (2014).

[19]J. W. Liu, M. Y. Liao, M. Imura, E. Watanabe, H. Oosato, and Y. Koide, Appl. Phys. Lett. **105**, 082110 (2014).

[20]J. Yang, F. Ren, Y. Chen, Y.-T. Liao, C.-W. Chang, J. Lin, Marko J. Tadjer, S. J. Pearton, and A. Kuramata, IEEE J. Electron Devices Soc. (unpublished).

[21]H. Umezawa, Mater. Sci. Semicond. Proc. **78**, 147 (2018).

[22]N. Izyumskaya, D. O. Demchenko, S. Das, Ü. Özgür, V. Avrutin, and H. Morkoç, Adv. Electron. Mater. **l.3**, 1600485 (2017).

[23]A. Nishikawa, K. Kumakura, T. Akasaka, and T. Makimoto, Appl. Phys. Lett. **88**, 173508 (2006).

[24]A. Nishikawa, K. Kumakura, and T. Makimoto, Jpn. J. Appl. Phys. **46**, 2316 (2007).

[25]R. J. Kaplar, A. A. Allerman, A. M. Armstrong, M. H. Crawford, J. R. Dickerson, A. J. Fischer, A. G. Baca, and E. A. Douglas, ECS J. Solid State Sci. Technol. **6**, Q3061 (2017).

[26]A. G. Baca, A. M. Armstrong, A. A. Allerman, E. A. Douglas, C. A. Sanchez, M. P. King, M. E. Coltrin, T. R. Fortune, and R. J. Kaplar, Appl. Phys. Lett. **109**, 033509 (2016).

[27]N. Yafune, S. Hashimoto, K. Akita, Y. Yamamoto, H. Tokuda, and M. Kuzuhara, Elec. Lett. **50**, 211 (2014).

[28]M. Higashiwaki, K. Sasaki, H. Murakami, Y. Kumagai, A. Koukitu, A. Kuramata, T. Masui, and S. Yamakoshi, Semicond. Sci. Technol. **31**, 034001 (2016).

[29]S. J. Pearton, J. Yang, P. H. Carey, IV, F. Ren, J. Kim, M. J. Tadjer, and M. A. Mastro, Appl. Phys. Rev. **5**, 011301 (2018).

[30]S. Okur, G. S. Tompa, N. Sbrockey, T. Salagaj, V. Blank, B. Henninger, M. Baldini, G. Wagner, Z. Galazka, Y. Yao, J. Rokholt, R. F. Davis, L. M. Porter, and A. Belkind, Vac. Technol. Coat. **5**, 31–39 (2017).

[31]M. H. Wong, K. Sasaki, A. Kuramata, S. Yamakoshi, and M. Higashiwaki, IEEE Electron Dev. Lett. **37**, 212 (2016).

[32]M. J. Tadjer, M. A. Mastro, N. A. Mahadik, M. Currie, V. D. Wheeler, J. A. Freitas, J. D. Greenlee, J. K. Hite, K. D. Hobart, C. R. Eddy, and F. J. Kub, J. Electron. Mater. **45**, 2031 (2016).

[33]M. A. Mastro, A. Kuramata, J. Calkins, J. Kim, F. Ren, and S. Pearton, ECS J. Solid State Sci. Technol. **6**, P356 (2017).

[34]C. A. Liechti, IEEE Trans. Microwave Theory Tech. **24**, 279 (1976).

[35]T. Sowlati, C. A. T. Salama, J. Sitch, G. Rabjohn, and D. Smith, IEEE J. Solid-State Circ. **30**, 1074 (1995).

[36]P. M. Solomon, Proc. IEEE **70**, 509 (1982).

[37]M. E. Kim, A. K. Oki, G. M. Gorman, D. K. Umemoto, and J. B. Camou, IEEE Trans. Microwave Theory Tech. **37**, 489 (1989).

[38]B. Bayraktaroglu, J. Barrette, L. Kehias, C. I. Huang, R. Fitch, R. Neidhard, and R. Scherer, IEEE Electron Dev. Lett. **14**, 493 (1993).

[39]See http://mil-embedded.com/articles/gan-tech-driving-radar-and-electronic-warfare-designs/ for details on use of GaN is self-driving cars.

[40]See https://www.electronicsweekly.com/news/5g-set-adopt-gan-military-protectionism-may-hit-supply-2018-02/ for discussion of export controls on GaN.

[41]See https://www.qorvo.com/applications/defense-aerospace for discussion of GaN defense and consumer applications.

[42]U. K. Mishra, L. Shen, T. E. Kazior, and Y.-F. Wu, Proc. IEEE **96**, 305 (2008).

[43]A. Shibib, L. Lorenz, and H. Ohashi, in *Proceedings of 30th International Symposium on Power Semiconductor Devices and ICs, Chicago, USA*, May, 2018 (IEEE, NY, 2018), pp. 1–7.

[44]L. Spaziani and L. Lu, "Silicon, GaN and SiC: There's room for all-an application space overview of device considerations," in *Proceedings of 30th International Symposium on Power Semiconductor Devices and ICs, Chicago, USA*, May, 2018 (IEEE, NY, 2018), pp. 8–11.

[45]A. Kuramata, K. Koshi, S. Watanabe, Y. Yamaoka, T. Masui, and S. Yamakoshi, Jpn. J. Appl. Phys. Part 1 **55**, 1202A2 (2016).

[46]Z. Galazka, R. Uecker, D. Klimm, K. Irmscher, M. Naumann, M. Pietsch, A. Kwasniewski, R. Bertram, S. Ganschow, and M. Bickermann, ECS J. Solid State Sci. Technol. **6**, Q3007 (2017).

[47]K. Hoshikawa, E. Ohba, T. Kobayashi, J. Yanagisawa, C. Miyagawa, and Y. Nakamura, J. Cryst. Growth **447**, 36 (2016).

[48]K. Sasaki, A. Kuramata, T. Masui, E. G. Víllora, K. Shimamura, and S. Yamakoshi, Appl. Phys. Express **5**, 035502 (2012).

[49]M. Baldini, M. Albrecht, A. Fiedler, K. Irmscher, R. Schewski, and G. Wagner, ECS J. Solid State Sci. Technol. **6**, Q3040 (2017).

[50]H. Murakami, K. Nomura, K. Goto, K. Sasaki, K. Kawara, Q. T. Thieu, R. Togashi, Y. Kumagai, M. Higashiwaki, A. Kuramata, S. Yamakoshi, B. Monemar, and A. Koukitu, Appl. Phys. Express **8**, 015503 (2015).

[51]Z. Xia, C. Joishi, S. Krishnamoorthy, S. Bajaj, Y. Zhang, M. Brenner, S. Lodha, and S. Rajan, IEEE Electron Device Letters **39**, 571 (2018)

[52]G. Wagner, M. Baldini, D. Gogova, M. Schmidbauer, R. Schewski, M. Albrecht, Z. Galazka, D. Klimm, and R. Fornari, Phys. Status Solidi A **211**, 27 (2014).

[53]J. R. Ritter, J. Huso, P. T. Dickens, J. B. Varley, K. G. Lynn, and M. D. McCluskey, Appl. Phys. Lett. **113**, 052101 (2018).

[54]T. Onuma, S. Saito, K. Sasaki, K. Goto, T. Masui, T. Yamaguchi, T. Honda, A. Kuramata, and M. Higashiwaki, Appl. Phys. Lett. **108**, 101904 (2016).

[55]M. Schubert, R. Korlacki, S. Knight, T. Hofmann, S. Schöche, V. Darakchieva, E. Janzén, B. Monemar, D. Gogova, Q.-T. Thieu, R. Togashi, H. Murakami, Y. Kumagai, K. Goto, A. Kuramata, S. Yamakoshi, and M. Higashiwaki, Phys. Rev. B **93**, 125209 (2016).

[56]N. Ma, N. Tanen, A. Verma, Z. Guo, T. Luo, H. Xing, and D. Jena, Appl. Phys. Lett. **109**, 212101 (2016).

[57]K. Ghosh and U. Singisetti, J. Appl. Phys. **122**, 035702 (2017).

[58]H. Peelaers, J. B. Varley, J. S. Speck, and C. G. Van de Walle, Appl. Phys. Lett. **112**, 242101 (2018).

[59]T. Kimoto and Y. Yonezawa, Mater. Sci. Semicond. Proc. **78**, 43 (2018).

[60]T. Yoshida, M. Imanishi, T. Kitamura, K. Otaka, M. Imade, M. Shibata, and Y. Mori, Phys. Status Solidi **254**, 1600671 (2017).

[61]T. Onuma, S. Fujioka, T. Yamaguchi, M. Higashiwaki, K. Sasaki, T. Masui, and T. Honda, Appl. Phys. Lett. **103**, 041910 (2013).

[62]Z. Galazka, K. Irmscher, R. Uecker, R. Bertram, M. Pietsch, A. Kwasniewski, M. Naumann, T. Schulz, R. Schewski, D. Klimm, and M. Bickermann, J. Cryst. Growth **404**, 184 (2014).

[63]M. Baldini, Z. Galazka, and G. Wagner, Mater. Sci. Semicond. Proc. **78**, 132 (2018).

[64]M. Higashiwaki, K. Sasaki, A. Kuramata, T. Masui, and S. Yamakoshi, Appl. Phys. Lett. **100**, 013504 (2012).

[65]K. Irmscher, Z. Galazka, M. Pietsch, R. Uecker, and R. Fornari, J. Appl. Phys. **110**, 063720 (2011).

[66]J. L. Hudgins, G. S. Simin, E. Santi, and M. A. Khan, IEEE Trans. Power Electron. **18**, 907 (2003).

[67]B. J. Baliga, J. Appl. Phys. **53**, 1759 (1982).

[68]E. O. Johnson, RCA Rev. **26**, 163 (1965).

[69]B. J. Baliga, IEEE Electron Dev. Lett. **10**, 455 (1989).

[70]B. J. Baliga, *Fundamentals of Power Semiconductor Devices*, 1st ed. (Springer, New York, 2010).

[71]W. Saito, Y. Takada, M. Kuraguchi, K. Tsuda, I. Omura, T. Ogura, and H. Ohashi, IEEE Trans. Electron Dev. **50**, 2528 (2003).

[72]K. Zeng, Y. Jia, and U. Singisetti, IEEE Electron Dev. Lett. **37**, 906 (2016).

[73]K. Zeng and U. Singisetti, Appl. Phys. Lett. **111**, 122108 (2017).

[74]F. Ejeckam, D. Francis, F. Faili, F. Lowe, J. Wilman, T. Mollart, J. Dodson, D. Twitchen, B. Bolliger, and D. Babic, "GaN on diamond: The next GaN," Microw. J. **5** (2014), see http://www.microwavejournal.com/articles/22161-gan-on-diamond-the-next-gan.

[75]C. Adams, "Beating the heat for emerging electronics," Avionics Today **7**, 31 (2018).

[76]P. Hindle, "Diamonds are a High-Power Engineer's Best Friend," Microw. J. **61**(6), 34 (2018), see http://www.microwavejournal.com/articles/30415-diamonds-are-a-high-power-engineers-best-friend.

[77]F. Ejeckam, D. Francis, F. Faili, D. J. Twitchen, B. Bolliger, J. Felbinger, and D. Babic, "GaN on diamond: A brief history," in *Lester Eastman Conference on High Performance Devices*, August 5–7, 2014. INSPEC Accession Number: 14775316.

[78]G. D. Via, J. G. Felbinger, J. Blevins, K. Chabak, G. Jessen, J. Gillespie, R. Fitch, A. Crespo, K. Sutherlin, B. Poling, S. Tetlak, R. Gilbert, T. Cooper, R. Baranyai, J. W. Pomeroy, M. Kuball, J. J. Maurer, and A. Bar-Cohen, in 10th International Conference on Nitride Semiconductors, Washington, DC, August 25–30, 2013.

[79]T. J. Anderson, K. D. Hobart, M. J. Tadjer, A. D. Koehler, E. A. Imhoff, J. K. Hite, T. I. Feygelson, B. B. Pate, C. R. Eddy, Jr., and F. J. Kub, ECS J. Solid State Sci. Technol. **6**, Q3036 (2017).

[80]F. Ejeckam, D. Babic, F. Faili, D. Francis, F. Lowe, Q. Diduck, C. Khandavalli, D. Twitchen, and B. Bolliger, in Semi Therm Conference, San Jose, CA, March 13, 2014.

[81]Q. Hao, H. Zhao, Y. Xiao, and M. B. Kronenfeld, Int. J. Heat Mass Transf. **116**, 496 (2018).

[82]L. Yates, A. Sood, Z. Cheng, T. Bougher, K. Malcom, J. Cho, M. Asheghi, K. Goodson, M. Goorsky, F. Faili, D. J. Twitchen, and S. Graham, "Characterization of the thermal conductivity of CVD diamond for GaN on diamond devices," in *Compound Semiconductor Integrated Circuit Symposium (CSICS)* (IEEE, 2016), pp. 1–4.

[83]D. H. Altman, A. Gupta, and M. Tyhach, "Development of a diamond microfluidics-based intra-chip cooling technology for GaN," in *ASME 2015 International Technical Conference and Exhibition on Packaging and Integration of Electronic and Photonic Microsystems, San Francisco, CA, USA*, July 6–9, 2015.

[84]J. W. Pomeroy, M. Singh, C. Middleton, M. J. Uren, M. H. Wong, K. Sasaki, A. Kuramata, S. Yamakoshi, M. Higashiwaki, and M. Kuball, in EMC Conference, Santa Barbara, CA, June 2018.

[85]Z. Liang, L. D. Martino, P. Ning, and F. Wang, US patent application, Pub. No.: US 2013/0020694 A1 (2013).

[86]See http://www.tamura-ss.co.jp/en/products/gao/index.html for a summary of available Gallium Oxide substrate and epitaxial wafers.

[87]A. Kyrtsos, M. Matsubara, and E. Bellotti, Appl. Phys. Lett. **112**, 032108 (2018).

[88]J. L. Lyons, Semicond. Sci. Technol. **33**, 05LT02 (2018).

[89]E. Chikoidze, A. Fellous, A. Perez-Tomas, G. Sauthier, C.-T. Tamar Tchelidze, T. T. Huynh, M. Phillips, S. Russell, M. Jennings, B. Berini, F. Jomard, and Y. Dumont, Mater. Today Phys. **3**, 118 (2017).

[90]T. Onuma, S. Saito, K. Sasaki, T. Masui, T. Yamaguchi, T. Honda, and M. Higashiwaki, Jpn. J. Appl. Phys. Part 1 **54**, 112601 (2015).

[91]S. Lany and A. Zunger, Phys. Rev. B **80**, 085202 (2009).

[92]J. Robertson and S. J. Clark, Phys. Rev. B **83**, 075205 (2011).

[93]D. O. Scanlon and G. W. Watson, J. Mater. Chem. **22**, 25236 (2012).

[94]J. B. Varley, A. Janotti, C. Franchini, and C. G. Van de Walle, Phys. Rev. B **85**, 081109 (2012).

[95]L. L. Liu, M. K. Li, D. Q. Yu, J. Zhang, H. Zhang, C. Qian, and Z. Yang, Appl. Phys. A **98**, 831 (2010).

[96]Q. Feng, J. Liu, Y. Yang, D. Pan, Y. Xing, X. Shi, X. Xia, and H. Liang, J. Alloys Compd. **687**, 964 (2016).

[97]S. S. Pan, G. H. Li, L. B. Wang, Y. D. Shen, Y. Wang, T. Mei, and X. Hu, Appl. Phys. Lett. **95**, 222112 (2009).

[98]K. H. L. Zhang, K. Xi, M. G. Blamire, and R. G. Egdell, J. Phys. Condens. Matter **28**, 383002 (2016).

[99]O. F. Schirmer, J. Phys. Condens. Matter **18**, R667 (2006).

[100]T. Zacherle, P. C. Schmidt, and M. Martin, Phys. Rev. B **87**, 235206 (2013).

[101]E. B. Yakimov, A. Y. Polyakov, N. B. Smirnov, I. V. Shchemerov, J. Yang, F. Ren, G. Yang, J. Kim, and S. J. Pearton, J. Appl. Phys. **123**, 185704 (2018).

[102]S. W. Kaun, F. Wu, and J. S. Speck, J. Vac. Sci. Technol. A **33**, 041508 (2015).

[103]P. Vogt and O. Bierwagen, Appl. Phys. Lett. **108**, 072101 (2016).

[104]E. Ahmadi, O. S. Koksaldi, S. W. Kaun, Y. Oshima, D. B. Short, U. K. Mishra, and J. S. Speck, Appl. Phys. Express **10**, 041102 (2017).

[105]S. Krishnamoorthy, Z. Xia, S. Bajaj, M. Brenner, and S. Rajan, Appl. Phys. Express **10**, 051102 (2017).

[106]R. Wakabayashi, T. Oshima, M. Hattori, K. Sasaki, T. Masui, A. Kuramata, S. Yamakoshi, K. Yoshimatsu, and A. Ohtomo, J. Cryst. Growth **424**, 77 (2015).

[107]T. Oshima, Y. Kato, N. Kawano, A. Kuramata, S. Yamakoshi, S. Fujita, T. Oishi, and M. Kasu, Appl. Phys. Express **10**, 035701 (2017).

[108]E. Ahmadi, O. S. Koksaldi, X. Zheng, T. Mates, Y. Oshima, U. K. Mishra, and J. S. Speck, Appl. Phys. Express **10**, 071101 (2017).

[109]S. Krishnamoorthy, Z. Xia, C. Joishi, Y. Zhang, J. McGlone, J. Johnson, M. Brenner, A. R. Arehart, J. Hwang, S. Lodha, and S. Rajan, Appl. Phys. Lett. **111**, 023502 (2017).

[110]T. Kawaharamura, G. T. Dang, and M. Furuta, Jpn. J. Appl. Phys. Part 1 **51**, 040207 (2012).

[111]T. Oshima, T. Nakazono, A. Mukai, and A. Ohtomo, J. Cryst. Growth **359**, 60 (2012).

[112]D. Tahara, H. Nishinaka, S. Morimoto, and M. Yoshimoto, Jpn. J. Appl. Phys. Part 1 **56**, 078004 (2017).

[113]M. Oda, R. Tokuda, H. Kambara, T. Tanikawa, T. Sasaki, and T. Hitora, Appl. Phys. Express **9**, 021101 (2016).

[114]T. Kamimura, D. Krishnamurthy, A. Kuramata, S. Yamakoshi, and M. Higashiwaki, Jpn. J. App. Phys. **55**, 1202B5 (2016).

[115]F. Alema, B. Hertog, A. Osinsky, P. Mukhopadhyay, M. Toporkov, and W. V. Schoenfeld, J. Cryst. Growth **475**, 77 (2017).

[116]S. Rafique, L. Han, A. T. Neal, S. Mou, M. J. Tadjer, R. H. French, and H. Zhao, Appl. Phys. Lett. **109**, 132103 (2016).

[117]D. Gogova, G. Wagner, M. Baldini, M. Schmidbauer, K. Irmscher, R. Schewski, and Z. Galazka, J. Cryst. Growth **401**, 665 (2014).

[118]Y. Yao, S. Okur, L. A. M. Lyle, G. S. Tompa, T. Salagaj, N. Sbrockey, R. F. Davis, and L. M. Porter, Mater. Res. Lett. **6**, 268 (2018).

[119]N. M. Sbrockey, T. Salagaj, E. Coleman, G. S. Tompa, Y. Moon, and M. S. Kim, J. Electron. Mater. **44**, 1357 (2015).

[120]Y. Oshima, E. G. Víllora, and K. Shimamura, Appl. Phys. Express **8**, 055501 (2015).

121H. Nishinaka, D. Tahara, S. Morimoto, and M. Yoshimoto, Mater. Lett. **205**, 28 (2017).

122F. Mezzadri, G. Calestani, F. Boschi, D. Delmonte, M. Bosi, and R. Fornari, Inorg. Chem. **55**, 12079 (2016).

123S. Yoshioka, H. Hayashi, A. Kuwabara, F. Oba, K. Matsunaga, and I. Tanaka, J. Phys. Condens. Matter **19**, 346211 (2007).

124M. Stavola and W. Beall Fowler, J. Appl. Phys. **123**, 161561 (2018).

125S. J. Pearton, J. W. Corbett, and M. Stavola, *Hydrogen in Crystalline Semiconductors* (Springer-Verlag, Heidelberg, 1992).

126J. B. Varley, A. Janotti, A. K. Singh, and C. G. Van de Walle, Phys. Rev. B **79**, 245206 (2009).

127A. T. Brant, S. Yang, N. C. Giles, and L. E. Halliburton, J. Appl. Phys. **110**, 053714 (2011).

128P. Weiser, M. Stavola, W. Beall Fowler, Y. Qin, and S. Pearton, Appl. Phys. Lett. **112**, 232104 (2018).

129S. Yang and L. E. Halliburton, Phys. Rev. B **81**, 035204 (2010).

130J. C. Yang, C. Fares, F. Ren, R. Sharma, E. Patrick, M. E. Law, S. J. Pearton, and A. Kuramata, J. Appl. Phys. **123**, 165706 (2018).

131B. E. Kananen, L. E. Halliburton, K. T. Stevens, G. K. Foundos, and N. C. Giles, Appl. Phys. Lett. **110**, 202104 (2017).

132E. Korhonen, F. Tuomisto, D. Gogova, G. Wagner, M. Baldini, Z. Galazka, R. Schewski, and M. Albrecht, Appl. Phys. Lett. **106**, 242103 (2015).

133B. E. Kananen, N. C. Giles, L. E. Halliburton, G. K. Foundos, K. B. Chang, and K. T. Stevens, J. Appl. Phys. **122**, 215703 (2017).

134A. Kyrtsos, M. Matsubara, and E. Bellotti, Phys. Rev. B **95**, 245202 (2017).

135M. E. Ingebrigtsen, J. B. Varley, A. Y. Kuznetsov, B. G. Svensson, G. Alfieri, A. Mihaila, U. Badstübner, and L. Vines, Appl. Phys. Lett. **112**, 042104 (2018).

136J. B. Varley, J. R. Weber, A. Janotti, and C. G. Van de Walle, Appl. Phys. Lett. **97**, 142106 (2010).

137P. Deak, Q. Duy Ho, F. Seeman, B. Aradi, M. Lorke, and T. Frauenheim, Phys. Rev. B **95**, 075208 (2017).

138Z. Zhang, E. Farzana, A. R. Arehart, and S. A. Ringel, Appl. Phys. Lett. **108**, 052105 (2016).

139M. Higashiwaki, K. Konishi, K. Sasaki, K. Goto, K. Nomura, Q. T. Thieu, R. Togashi, H. Murakami, Y. Kumagai, B. Monemar, A. Koukitu, A. Kuramata, and S. Yamakoshi, Appl. Phys. Lett. **108**, 133503-1-4 (2016).

140J. Yang, S. Ahn, F. Ren, S. J. Pearton, S. Jang, J. Kim, and A. Kuramata, Appl. Phys. Lett. **110**, 192101 (2017).

141J. Yang, S. Ahn, F. Ren, S. J. Pearton, S. Jang, and A. Kuramata, IEEE Electron Dev. Lett. **38**, 906 (2017).

142K. Konishi, K. Goto, H. Murakami, Y. Kumagai, A. Kuramata, S. Yamakoshi, and M. Higashiwaki, Appl. Phys. Lett. **110**, 103506 (2017).

143M. J. Tadjer, A. D. Koehler, N. A. Mahadik, E. Glaser, J. A. Freitas, B. Feigelson, V. D. Wheeler, K. D. Hobart, F. J. Kub, and A. Kuramata, Thick, low-doped homoepitaxial Ga$_2$O$_3$ for power electronics applications, in *232nd ECS Meeting, National Harbor, MD, October 2017*.

144H. Fu, H. Chen, X. Huang, I. Baranowski, J. Montes, T.-H. Yan, and Y. Zhao, IEEE Trans. Electron Dev. **65**(8), 3507–3513 (2018), see https://arxiv.org/ftp/arxiv/papers/1712/1712.01318.pdf.

145J. Bae, H. W. Kim, I. H. Kang, G. Yan, and J. Kim, Appl. Phys. Lett. **112**, 122102-1-4 (2018).

146T. Oishi, Y. Koga, K. Hara, and M. Kasu, Appl. Phys. Express **8**, 31101-1-7 (2015).

147S. Oh, G. Yang, and J. Kim, ECS J. Solid State Sci. Technol. **6**, Q3022 (2017).

148K. Nakai, T. Nagai, K. Noami, and T. Futagi, Jpn. J. Appl. Phys. **54**, 051103 (2015).

149K. Hanada, T. Moribayashi, K. Koshi, K. Sasaki, A. Kuramata, O. Ueda, and M. Kasu, Jpn. J. Appl. Phys. **55**, 1202BG (2016).

150M. Kasu, K. Hanada, T. Moribayashi, A. Hashiguchi, T. Oshima, T. Oishi, K. Koshi, K. Sasaki, A. Kuramata, and O. Ueda, Jpn. J. Appl. Phys. **55**, 1202BB-1-4 (2016).

151T. Oshima, A. Hashiguchi, T. Moribayashi, K. Koshi, K. Sasaki, A. Kuramata, O. Ueda, T. Oishi, and M. Kasu, Jpn. J. Appl. Phys. **56**, 086501 (2017).

152O. Ueda, N. Ikenaga, K. Koshi, A. Kuramata, T. Moribayashi, S. Yamakoshi, K. Hanada, and M. Kasu, Jpn. J. Appl. Phys. **55**, 1202BD (2016).

153M. Kasu, T. Oshima, K. Hanada, T. Moribayashi, A. Hashiguchi, T. Oishi, K. Koshi, K. Sasaki, A. Kuramata, and O. Ueda, Jpn. J. Appl. Phys. **56**, 091101-1-5 (2017).

154J. H. Choi, C. H. Cho, and H. Y. Cha, Res. Phys. **9**, 1170 (2018).

155M. J. Tadjer, N. A. Mahadik, J. A. Freitas, E. R. Glaser, A. D. Koehler, L. E. Luna, B. N. Feigelson, K. D. Hobart, F. J., Kub, and A. Kuramata, "Ga$_2$O$_3$ Schottky barrier and heterojunction diodes for power electronics applications," Proc. SPIE **10532**, 1053212 (2018),

156J. C. Yang, F. Ren, M. J. Tadjer, S. J. Pearton, and A. Kuramata, AIP Adv. **8**, 055026 (2018).

157J. C. Yang, F. Ren, M. J. Tadjer, S. J. Pearton, and A. Kuramata, ECS J. Solid State Sci. Technol. **7**, Q92 (2018).

158J. C. Yang, F. Ren, M. J. Tadjer, S. J. Pearton, and A. Kuramata, IEEE Trans. Electron Dev. **65**, 2790 (2018).

159C. Joishi, S. Rafique, Z. Xia, L. Han, S. Krishnamoorthy, Y. Zhang, L. Lodha, H. Zhao, and S. Rajan, Appl. Phys. Express **11**, 031101-1-5 (2018).

160V. Kumar, G. Chen, S. Guo, and I. Adesida, IEEE Trans. Electron Dev. **53**, 1477 (2006).

161A. Chini, D. Buttari, R. Coffie, L. Shen, S. Heikman, A. Chakraborty, S. Keller, and U. Mishra, IEEE Electron Dev. Lett. **25**, 229 (2004).

162W. Li, Q. Wang, X. Zhan, J. Yan, L. Jiang, H. Yin, J. Gong, X. Wang, F. Liu, and B. Li, Semicond. Sci. Technol. **31**, 125003 (2016).

163H. Xing, Y. Dora, A. Chini, S. Heikman, S. Keller, and U. Mishra, IEEE Electron Dev. Lett. **25**, 161 (2004).

164Y. Kokubun, K. Miura, F. Endo, and S. Nakagomi, Appl. Phys. Lett. **90**, 031912 (2007).

165R. Suzuki, S. Nakagomi, and Y. Kokubun, Appl. Phys. Lett. **98**, 131114 (2011).

166S.-Y. Sung, S.-Y. Kim, K.-M. Jo, J.-H. Lee, J.-J. Kim, S.-G. Kim, K.-H. Chai, S. J. Pearton, D. P. Norton, and Y.-W. Heo, Citation Appl. Phys. Lett. **97**, 222109 (2010).

167M. Grundmann, F.-L. Schein, M. Lorenz, T. Böntgen, J. Lenzner, and H. von Wenckstern, Phys. Status Solidi A **210**, 1671 (2013).

168K. Kaneko, S. Fujita, and T. Hitora, Jpn. J. Appl. Phys. **57**, 02CB18 (2018).

169R. Raghunathan and B. J. Baliga, Appl. Phys. Lett. **72**, 3196 (1998).

170A. P. Zhang, G. Dang, F. Ren, H. Cho, K. Lee, S. J. Pearton, J. I. Chyi, T. Nee, C. Lee, and C. Chuo, IEEE Trans. Electron. Dev. **48**, 407 (2001).

171P. G. Neudeck, D. J. Spry, L. Chen, N. F. Prokop, and M. J. Krasowski, IEEE Electron Dev. Lett. **38**(8), 1082 (2017).

172D. J. Spry, P. G. Neudeck, D. Lukco, L. Chen, M. J. Krasowski, N. F. Prokop, C. W. Chang, and G. M. Beheim, Mater. Sci. Forum **924**, 949–952 (2018).

173A. F. Witulski, D. R. Ball, K. F. Galloway, A. Javanainen, J.-M. Lauenstein, A. L. Sternberg, and R. D. Schrimpf, IEEE Trans. Nucl. Sci. **65**(8), 1951 (2018).

174G. H. Johnson, J. H. Hohl, R. D. Schrimpf, and K. F. Galloway, IEEE Trans. Electron Dev. **40**(5), 1001 (1993).

175C. Delfaure, M. Pomorski, J. de Sanoit, P. Bergonzo, and S. Saada, Appl. Phys. Lett. **108**, 252105 (2016).

176F. Ricci, F. Boschi, A. Baraldi, A. Filippetti, M. Higashiwaki, A. Kuramata, V. Fiorentini, and R. Fornari, J. Phys. Condens. Matter **28**, 224005 (2016).

177P. Jiang, X. Qian, X. Li, and R. Yang, "Three-dimensional anisotropic thermal conductivity tensor of single crystalline β-Ga$_2$O$_3$" (unpublished).

178A. Mock, R. Korlacki, C. Briley, V. Darakchieva, B. Monemar, Y. Kumagai, K. Goto, M. Higashiwaki, and M. Schubert, Phys. Rev. B **96**, 245205 (2017).

179K. Ghosh and U. Singisetti, J. Appl. Phys. **124**, 085707 (2018).

180Y. Zhang, A. Neal, Z. Xia, C. Joishi, J. M. Johnson, Y. Zheng, S. Bajaj, M. Brenner, D. Dorsey, K. D. Chabak, G. Jessen, J. Hwang, S. Mou, J. P. Heremans, and S. Rajan, Appl. Phys. Lett. **112**, 173502 (2018).

181M. H. Wong, K. Goto, Y. Morikawa, A. Kuramata, S. Yamakoshi, H. Murakami, Y. Kumagai, and M. Higashiwaki, Appl. Phys. Express **11**, 064102 (2018).

182Z. Hu, K. Nomoto, W. Li, N. Tanen, K. Sasaki, A. Kuramata, T. Nakamura, D. Jena, and H. G. Xing, IEEE Electron Dev. Lett. **39**(6), 869 (2018).

183Y. Lv, X. Zhou, S. Long, X. Song, Y. Wang, S. Liang, Z. He, T. Han, X. Tan, Z, Feng, H. Dong, X. Zhou, Y. Yu, S. Cai, and M. Liu, IEEE Electron Device Lett. (unpublished).

184M. H. Wong, C. H. Lin, A. Kuramata, S. Yamakoshi, H. Murakami, Y. Kumagai, and M. Higashiwaki, Appl. Phys. Lett. **113**, 102103 (2018).

[185]K. Sasaki, paper presented at International Conference on SiC and Related Materials (ICSCRM), Washington D. C. 2017.

[186]A. T. Neal, S. Mou, S. Rafique, H. Zhao, E. Ahmadi, J. S. Speck, K. T. Stevens, J. D. Blevins, D. B. Thomson, N. Moser, K. D. Chabak, and G. H. Jessen, Appl. Phys. Lett. **113**, 062101 (2018).

[187]N. Moser, J. McCandless, A. Crespo, K. Leedy, A. Green, A. Neal, S. Mou, E. Ahmadi, J. Speck, K. Chabak, N. Peixoto, and G. Jessen, IEEE Electron Dev. Lett. **38**, 775 (2017).

[188]K. D. Leedy, K. D. Chabak, V. Vasilyev, D. C. Look, J. J. Boeckl, J. L. Brown, S. E. Tetlak, A. J. Green, N. A. Moser, A. Crespo, D. B. Thomson, R. C. Fitch, J. P. McCandless, and G. H. Jessen, Appl. Phys. Lett. **111**, 012103 (2017).

[189]H. Bae, Jinhyun Noh, S. Alghamdi, M. Si, and P. D. Ye, IEEE Electron Dev. Lett. **39**, 1708 (2018).

[190]M. A. Bhuiyan, H. Zhou, R. Jiang, E. X. Zhang, D. M. Fleetwood, P. D. Ye, and T.-P. Ma, IEEE Electron Dev. Lett. **39**, 1022 (2018).

[191]K. Zeng, A. Vaidya, and U. Singisetti, IEEE Electron Dev. Lett. **39**, 1385 (2018).

[192]K. Zeng, Y. Jia, and U. Singisetti, IEEE Electron Dev. Lett. **37**, 906 (2016).

[193]N. Ma, N. Tanen, A. Verma, Z. Guo, T. Luo, H. Xing, and D. Jena, Appl. Phys. Lett. **109**, 212101 (2016).

[194]H. Yamaguchi and A. Kuramata, J. Appl. Cryst. **51** (2018).

[195]M. H. Wong, Y. Morikawa, K. Sasaki, A. Kuramata, S. Yamakoshi, and M. Higashiwaki, Appl. Phys. Lett. **109**, 193503 (2016).

[196]M. Singh, M. A. Casbon, M. J. Uren, J. W. Pomeroy, S. Dalcanale, S. Karboyan, P. J. Tasker, M. H. Wong, K. Sasaki, A. Kuramata, S. Yamakoshi, M. Higashiwaki, and M. Kuball, IEEE Electron Dev. Lett. **39**(10), 1572–1575 (2018).

[197]M. J. Tadjer, N. A. Mahadik, V. D. Wheeler, E. R. Glaser, L. Ruppalt, A. D. Koehler, K. D. Hobart, C. R. Eddy, and F. J. Kub, ECS J. Solid State Sci. Technol. **5**, P468 (2016).

[198]A. J. Green, K. D. Chabak, E. R. Heller, R. C. Fitch, M. Baldini, A. Fiedler, K. Irmscher, G. Wagner, Z. Galazka, S. E. Tetlak, A. Crespo, K. Leedy, and G. H. Jessen, IEEE Electron Dev. Lett. **37**, 902 (2016).

[199]N. A. Moser, J. P. McCandless, A. Crespo, K. D. Leedy, A. J. Green, E. R. Heller, K. D. Chabak, N. Peixoto, and G. H. Jessen, Appl. Phys. Lett. **110**, 143505 (2017).

[200]M. Higashiwaki, K. Sasaki, T. Kamimura, M. Hoi Wong, D. Krishnamurthy, A. Kuramata, T. Masui, and S. Yamakoshi, Appl. Phys. Lett. **103**, 123511 (2013).

[201]Z. Hu, K. Nomoto, W. Li, N. Tanen, K. Sasaki, A. Kuramata, T. Nakamura, D. Jena, and H. G. Xing, IEEE Electron Dev. Lett. **39**, 869 (2018).

[202]K. D. Chabak, N. Moser, A. J. Green, D. E. Walker, S. E. Tetlak, E. Heller, A. Crespo, R. Fitch, J. P. McCandless, K. Leedy, M. Baldini, G. Wagner, Z. Galazka, X. Li, and G. Jessen, Appl. Phys. Lett. **109**, 213501 (2016).

[203]M. H. Wong, Y. Nakata, A. Kuramata, S. Yamakoshi, and M. Higashiwaki, Appl. Phys. Express **10**, 041101 (2017).

[204]K. Sasaki, Q. T. Thieu, D. Wakimoto, Y. Koishikawa, A. Kuramata, and S. Yamakoshi, Appl. Phys. Express **10**, 124201 (2017).

[205]A. J. Green, K. D. Chabak, M. Baldini, N. Moser, R. Gilbert, R. C. Fitch, G. Wagner, Z. Galazka, J. McCandless, A. Crespo, K. Leedy, and G. H. Jessen, IEEE Electron Dev. Lett. **38**, 790 (2017).

[206]K. Zeng, J. S. Wallace, C. Heimburger, K. Sasaki, A. Kuramata, T. Masui, J. A. Gardella, and U. Singisetti, IEEE Electron Dev. Lett. **38**, 513 (2017).

[207]H. Zhou, K. Maize, G. Qiu, A. Shakouri, and P. D. Ye, Appl. Phys. Lett. **111**, 092102 (2017).

[208]H. Zhou, M. Si, S. Alghamdi, G. Qiu, L. Yang, and P. D. Ye, IEEE Electron Dev. Lett. **38**, 103 (2017).

[209]Z. Hu, K. Nomoto, W. Li, L. J. Zhang, J.-H. Shin, N. Tanen, T. Nakamura, D. Jena, and H. G. Xing, "Vertical fin Ga2O power field-effect transistors with on/off ratio > 109," in *75th Annual IEEE Device Research Conference (DRC)* (IEEE, 2017), pp. 1–2.

[210]J. Yang, S. Sparks, F. Ren, S. J. Pearton, and M. Tadjer, J. Vac. Sci. Technol. B **36**, 061201 (2018).

[211]Y. Jia, K. Zeng, J. S. Wallace, J. A. Gardella, and U. Singisetti, Appl. Phys. Lett. **106**, 102107 (2015).

[212]K. Konishi, T. Kamimura, M. H. Wong, K. Sasaki, A. Kuramata, S. Yamakoshi, and M. Higashiwaki, Phys. Status Solidi B **253**, 623 (2016).

[213]P. H. Carey, IV, F. Ren, D. C. Hays, B. P. Gila, S. J. Pearton, S. Jang, and A. Kuramata,: Jpn. J. Appl. Phys. **56**, 071101 (2017).

[214]T. H. Hung, K. Sasaki, A. Kuramata, D. N. Nath, P. S. Park, C. Polchinski, and S. Rajan, Appl. Phys. Lett. **104**, 162106 (2014).

[215]T. Kamimura, K. Sasaki, M. H. Wong, D. Krishnamurthy, A. Kuramata, T. Masui, S. Yamakoshi, and M. Higashiwaki, Appl. Phys. Lett. **104**, 192104 (2014).

[216]P. H. Carey, IV, F. Ren, D. C. Hays, B. P. Gila, S. J. Pearton, S. Jang, and A. Kuramata, Vacuum **142**, 52 (2017).

[217]M. Kim, J. H. Seo, U. Singisetti, and Z. Ma, J. Mater. Chem. C **5**, 8338 (2017).

[218]A. F. Basile, J. Rozen, J. R. Williams, L. C. Feldman, and P. M. Mooney, J. Appl. Phys. **109**, 064514 (2011).

[219]J. Tan, M. K. Das, J. A. Cooper, Jr., and M. R. Melloch, Appl. Phys. Lett. **70**, 2280 (1997).

[220]P. Fiorenza, A. Frazzetto, A. Guarnera, M. Saggio, and F. Roccaforte, Appl. Phys. Lett. **105**, 142108 (2014).

[221]H. F. Li, S. Dimitrijev, H. B. Harrison, and D. Sweatman, Appl. Phys. Lett. **70**, 2028 (1997).

[222]G. Liu, A. C. Ahyi, Y. Xu, T. Isaacs-Smith, Y. K. Sharma, J. R. Williams, L. C. Feldman, and S. Dhar, IEEE Electron Dev. Lett. **34**, 181 (2013).

[223]R. Zou, Z. Zhang, Q. Liu, J. Hu, L. Sang, M. Liao, and W. Zhang, Small **10**, 1848 (2014).

[224]J. Kim, S. Oh, M. A. Mastro, and J. Kim, Phys. Chem. Chem. Phys. **18**, 15760 (2016).

[225]S. Ahn, F. Ren, J. Kim, S. Oh, J. Kim, M. A. Mastro, and S. Pearton, Appl. Phys. Lett. **109**, 062102 (2016).

[226]G. Yang, S. Jang, F. Ren, S. J. Pearton, and J. Kim, ACS Appl. Mater. Interfaces **9**, 40471 (2017).

[227]S. Oh, M. A. Mastro, M. J. Tadjer, and J. Kim, ECS J. Solid State Sci. Technol. **6**, Q79 (2017).

[228]R. Mitdank, S. Dusari, C. Bülow, M. Albrecht, Z. Galazka, and S. Fischer, Phys. Status Solidi A **211**, 543 (2014).

[229]W. S. Hwang, A. Verma, H. Peelaers, V. Protasenko, S. Rouvimov, H. Xing, A. Seabaugh, W. Haensch, C. V. de Walle, and Z. Galazka, Appl. Phys. Lett. **104**, 203111 (2014).

[230]A. Castellanos-Gomez, M. Buscema, R. Molenaar, V. Singh, L. Janssen, H. S. J. van dar Zant, and G. A. Steele, 2D Mater. **1**, 011002 (2014).

[231]Y. Kwon, G. Lee, S. Oh, J. Kim, S. J. Pearton, and F. Ren, Appl. Phys. Lett. **110**(13), 131901 (2017).

[232]J. Kim, M. A. Mastro, M. J. Tadjer, and J. Kim, ACS Appl. Mater. Interfaces **10**(35), 29724 (2018).

[233]J. Bae, H. W. Kim, I. H. Kang, G. Yang, and J. Kim, Appl. Phys. Lett. **112**, 122102 (2018).

[234]S. Oh, C.-K. Kim, and J. Kim, ACS Photonics **5**, 1123 (2018).

[235]M. Handwerg, R. Mitdank, Z. Galazka, and S. F. Fischer, Semicond Sci. Technol. **31**, 125006 (2016).

[236]M. Handwerg, R. Mitdank, Z. Galazka, and S. F. Fischer, Semicond. Sci. Technol. **30**, 024006 (2015).

[237]M. D. Santia, N. Tandon, and J. D. Albrecht, Appl. Phys. Lett. **107**, 041907 (2015).

[238]Z. Guo, A. Verma, X. Wu, F. Sun, A. Hickman, T. Masui, A. Kuramata, M. Higashiwaki, D. Jena, and T. Luo, Appl. Phys. Lett. **106**, 111909 (2015).

[239]C.-H. Lin, N. Hatta, K. Konishi, S. Watanabe, A. Kuramata, K. Yagi, and M. Higashiwaki, in EMC Conference, Santa Barbara, CA, June 2018.

[240]Z. Yan and S. Kumar, in EMC Conference, Santa Barbara, CA, June 2018.

[241]See, for example, applications for GaN in renewable energy and automotive applications at https://gansystems.com/market-insights/?utm_source = hmpg-slider.

[242]B. Bayraktaroglu, Assessment of Gallium Oxide Technology, Devices for Sensing Branch Aerospace Components & Subsystems Division, AFRL-RY-WP-TR-2017-0167, August 2017, see http://www.dtic.mil/dtic/tr/fulltext/u2/1038137.pdf.

[243]A. V. Sumant and J. E. Butler, "The CVD of nanodiamond materials," Chem. Vap. Deposition **14**, 145–160 (2008).

[244]SEMICON Europa, From 13 November 2018–16 November 2018, see http://www.semiconeuropa.org/.

[245]Yole Development http://www.yole.fr/Reports.aspx on power SiC device insertion into applications, ie. https://www.i-micronews.com/compound-semi-report/product/power-sic-2018-materials-devices-and-applications.html and also on power electronics prospects for electric vehicle charging, ie. https://www.i-micronews.com/category-listing/product/power-electronics-for-ev-hev-2018.html.

[246]F. Ejeckam, in *Proceedings of the Lester Eastman Conference on High Performance Devices* (IEEE, 2014), and references therein.

[247]J. Noh, M. Si, H. Zhou, M. J. Tadjer, and P. D. Ye, in 76th *Device Research Conference Proceedings* (IEEE, 2018).

[248]M. J. Tadjer, T. J. Anderson, J. C. Gallagher, P. E. Raad, P. Komarov, A. D. Koehler, K. D. Hobart, and F. J. Kub, in *76th Device Research Conference Proceedings* (IEEE, 2018).

[249]See http://www.jcnnewswire.com/japanese/pressrelease/40176/3/Fujitsu-Technology-Bonds-Single-crystal-Diamond-and-SiC-at-Room-Temperature-Enables-Boost-to-Radar-Performance, for a discussion of use of diamond heat sinks enabling higher power performance.

[250]C. Yang, M. Kneis, M. Lorenz, and M. Grundmann, Proc. Natl. Acad Sci. U.S.A. **113**, 12929 (2016).

[251]N. Yamada, R. Ino, and Y. Ninomiya, "Truly transparent p-type γ-CuI thin films with high hole mobility," Chem. Mater. **28**, 4971 (2016).

[252]M. Grundmann, F. Klüpfel, R. Karsthof, P. Schlupp, F.-L. Schein, D. Splith, C. Yang, S. Bitter, and H. von Wenckstern, "Oxide bipolar electronics: Materials, devices and circuits," J. Phys. D **49**, 213001 (2016).

[253]M. J. Tadjer, L. E. Luna, E. Cleveland, K. D. Hobart, and F. J. Kub, ECS Trans. **85**, 21 (2018).

[254]A. Liu, H. Zhu, W.-T. Park, S.-J. Kang, Y. Xu, M.-G. Kim, and Y.-Y. Noh, Adv. Mater. 30, 1802379 (2018).

[255]Y. Kokubun, S. Kubo, and S. Nakagomi, Appl. Phys. Express **9**, 091101 (2016).

[256]T. Watahiki, Y. Yuda, A. Furukawa, M. Yamamuka, Y. Takiguchi, and S. Miyajima, Appl. Phys. Lett. **111**, 222104 (2017).

[257]M. J. Tadjer, "Cheap ultra-wide bandgap power electronics? Gallium oxide may hold the answer," ECS Interfaces (in press).

[258]Z. Hu, K. Nomoto, W. Li, Z. Zhang, N. Tanen, Q. T. Thieu, K. Sasaki, A. Kuramata, T. Nakamura, D. Jena, and H. G. Xing, Appl. Phys. Lett. **113**, 122103 (2018).

[259]A. Takatsuka, K. Sasaki, D. Wakimoto, Q. T. Thieu, Y. Koishikawa, J. Arima, J. Hirabayashi, D. Inokuchi, Y. Fukumitsu, A. Kuramata, and S. Yamakoshi, "Fast recovery performance of β-Ga₂O₃ Trench MOS Schottky barrier diodes," in *2018 76th Device Research Conference (DRC)*, *June 2018* (IEEE, 2018), pp. 1–2.

[260]Q. He, W. Mu, B. Fu, Z. Jia, S. Long, Z. Yu, Z. Yao, W. Wang, H. Dong, Y. Qin, G. Jian, Y. Zhang, H. Xue, H. Lv, Q. Liu, M. Tang, X. Tao, and M. Liu, IEEE Electron. Dev. Lett **39**, 556 (2018).

[261]I. Lee, A. Kumar, K. Zeng, U. Singisetti, and X. Yao, "Mixed-mode circuit simulation to characterize Ga₂O₃ MOSFETs in different device structures", in *2017 IEEE 5th Workshop on Wide Bandgap Power Devices and Applications (WiPDA)* (IEEE, 2017), pp. 185–189.

[262]X. H. Wen, H. Q. Ming, J. G. Zhong, L. S. Bing, P. Tao, and L. Ming, Nanoscale Res. Lett. **13**, 290 (2018).

[263]R. Eden, GaN data from SiC and GaN Power Semiconductors Report—2016 (IHS), Silicon Carbide & Gallium Nitride Power Semiconductors, 2016, see https://technology.ihs.com/521146/sic-gan-power-semiconductors-2016.

[264]Diamond data from U.S. Department of Energy. "Wide bandgap semiconductors for power electronics," in *Quadrennial Technology Review 2016* (2015), see http://energy.gov/sites/prod/files/2015/09/f26/QTR2015-06-Manufacturing.pdf.

[265]Geological Survey, Report on Diamond (Industrial), 2016, see http://minerals.usgs.gov/minerals/pubs/commodity/diamond/mcs-2016-diamo.pdf.